From Lewis, Cleveland

NAG 3-530

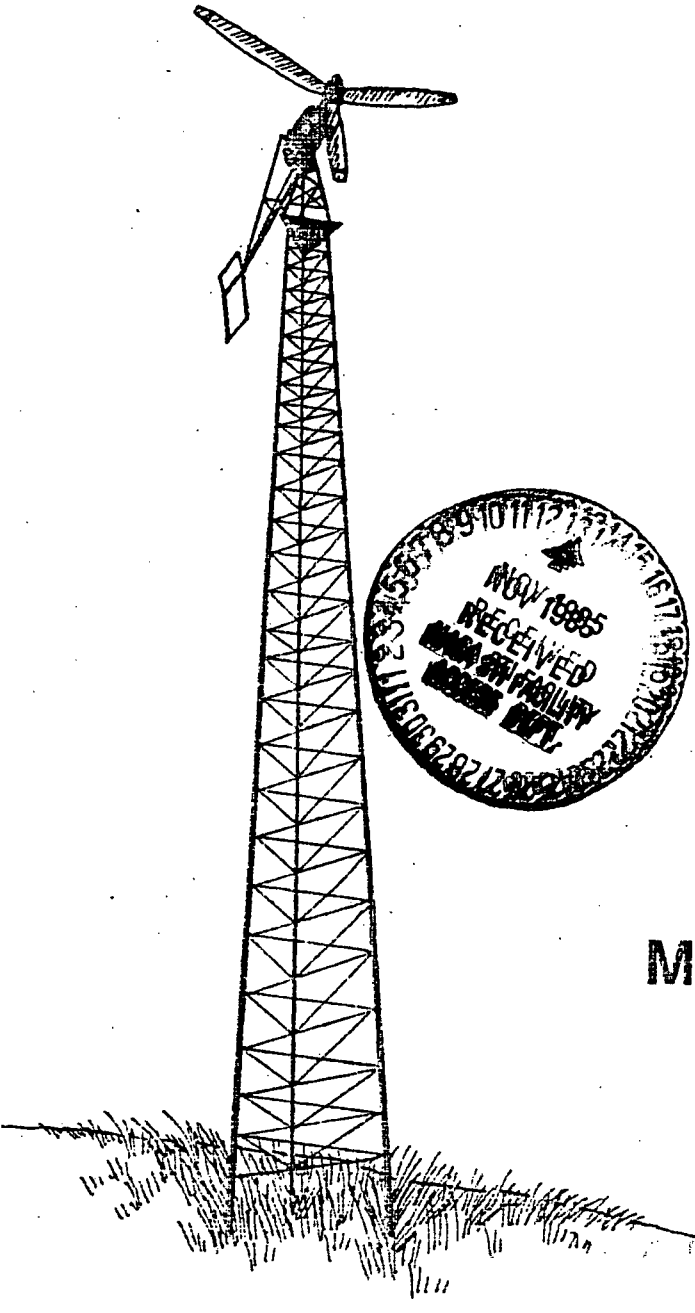

AC MOTOR AND GENERATOR REQUIREMENTS FOR ISOLATED WECS

G. L. PARK

P. J. MCCLEER

B. HANSON

B. WEINBERG

O. KRAUSS

Michigan State University

Division of Engineering Research

October, 1985

DOE/NASA/0530-1
NASA CR-176315

AC MOTOR AND GENERATOR REQUIREMENTS FOR ISOLATED WECS

Gerald L. Park, Principal Investigator, Michigan State University
Patrick J. McCleer, University of Michigan
Bror Hanson, SWX Corp.
Bernhard Weinberg, Michigan State University
Otto Krauss, Michigan State University

October, 1985

Prepared for
NATIONAL AERONAUTICS AND SPACE ADMINISTRATION
Lewis Research Center
Cleveland, Ohio 44135
Under Grant NAG 3-530

for
U.S. DEPARTMENT OF ENERGY
Conservation and Renewable Energy
Wind Energy Technology Division
Under Interagency Agreement

The University of Michigan and SWX Corp. were subcontractors to the Division of Engineering Research at Michigan State University

TABLE OF CONTENTS

ABSTRACT

After surveying electrically-driven loads used on productive farms, the investigators chose three pumps for testing at voltages and frequencies far outside the normal operating range. These loads extract and circulate water and move heat via air, and all are critical to farm productivity. The object was to determine the envelope of supply voltage and frequency over which these loads would operate stably for time intervals under 1 hour. This information is among that needed to determine the feasibility of supplying critical loads, in case of a utility outage, from a wind-driven alternator whose output voltage and frequency will vary dramatically in most continental wind regimes.

The report surveys other related work, describes the salient features and limitations of the test configurations used, describes the data reduction, and outlines the development of simulation models suitable for a small computer. The results are primarily displayed on the voltage-frequency plane with the general conclusion that the particular pump models considered will operate over the range of 50 to 90 Hz and a voltage band which starts below rated, decreases as frequency decreases, and is limited on the high side by excessive motor heating. For example, centrifugal pump operating voltage ranges as extensive .4 to 1.4 pu appear possible.

Particular problems with starting, stalling due to lack of motor torque, high speed cavitation, and likely overheating are addressed in a listing of required properties for wind-driven alternators and their controllers needed for use in the isolated or stand-alone configuration considered.

LIST OF FIGURES AND TABLES

I. INTRODUCTION AND PROBLEM STATEMENT

Before reliable utility electric service was widely available on farms, non-vehicular mechanical power was provided by other sources including mechanical hydro power for grinding, wind-driven pumps for water supply, and draft animals harnessed to lift water for irrigation. Reliable electric motors displaced these sources and have made a significant contribution to agricultural productivity. However, there is a small possibility of long-term utility outages, due to fuel shortages or disaster. Could alternative sources then continue farm production when utility electric energy is unavailable or too expensive to deliver to remote sites? This report is a preliminary step towards the answer.

Although a complete list of electrical farm equipment is extensive, there are several motor loads necessary to almost all farming operations. They include water pumping and circulation for animal, crop, and residential needs. Cooling and heating, while not necessary in some farm operations, is needed for rural residences as well as for dairy operations.

The alternative source considered in this study is wind energy as converted by variable-speed self-excited alternators—a practical wind energy alternative not requiring utility power for excitation or control. The common wind-driven induction generator is currently practical only when excited by a strong outside source. Photovoltaic sources would require a force-commutated DC to AC inverter designed for isolated operation since farm motors are all AC and designed for nominal utility service voltages and 60 Hz. Fueled auxiliary generators can provide near utility-grade energy and present few new technical problems for evaluation when the load is nearly constant.. In addition, during a prolonged utility outage, that fuel could instead be used for farm vehicles if wind energy was available.

A stand-alone wind-driven alternator, without extensive and expensive controls, will vary unpredictably and substantially (4 to 1) in speed (and thus frequency) and in terminal voltage as wind velocity and load demand vary. Thus, any load connected to such a source must operate over a voltage-frequency range (envelope) far in excess of normal load design conditions. The latter are usually 60 Hz $\pm$ 5%, and 120, 240, or 480 volts + 5%. Although AC motors can be manufactured to operate over a wider range of input conditions, the cost may be excessive given the low risk of an extended utility outage. In other words, why retrofit existing electric drives with expensive wide-range motors for use with a new windmill when the extra range is needed only for a low-probability prolonged outage? Perhaps it is better to augment the controls of a wind-driven alternator so its output can drive standard motors designed for small variations in frequency and voltage under the much greater voltage and frequency deviations present in isolated operation.

The essence of this problem is: Find the operating envelope in voltage and frequency of several critical motor-driven farm loads and find the properties of the controller of an alternator windmill to enable it to operate these loads outside design conditions without immediate damage. Although a motor and load may appear to operate satisfactorily for a short time outside the design envelope, extended operation under such conditions may reduce service

life and increase maintenance costs. For example, temperature rise and vibration limits may be exceeded. If extensive off-design operation is anticipated, these conditions should be investigated. A thorough exploration of this problem was far beyond the time and resources available under this grant so the effort was simplified.

> A useful first step is finding the short-term (several minute) steady-state operating envelope of three common and commercially available farm pumping loads for frequencies between 40 and 100 hz and for voltages ranging across and far outside the manufacturers specifications.

A field feasibility study, including limited testing, as opposed to a controlled lab investigation, was intended. There were some limitations. For example, shaft torque and speed were impossible to measure directly due to pump-motor packaging and location charateristic of these commonly used pumps. Computer simulations were then used to compare with test results and together they suggest windmill controller characteristics for isolated steady-state operation of these critical loads. Future work is needed to investigate service life, transient conditons like motor starting and sudden load changes, and the effect of these loads on the behavior of wind turbine generators.

II. RELATED WORK

Many modern textbooks on electric machines [eg: Ref. 1 and 11] include development of circuit and dynamic models applicable to caged induction motors operating over a wide range of supply voltage and frequency. The emergence of a substantial market for solid-state variable-speed induction motor drives is testimony that motors can successfully operate over a wider range of supply conditions than is suggested by the motor nameplates. The specification sheets provided by manufacturers for various classes of caged-rotor motors list the effects of 10% voltage and 5% frequency changes on motor torque, current, speed, power factor, efficiency and temperature rise. For example, one line of integral horsepower drip-proof motors is said to decrease torque by 10%, increase speed by 5%, and "slightly increase" efficiency for a 5% frequency increase.

Although a literature search was not part of this study, the investigators are not aware of an extensive literature reporting on large changes in supply parameters for farm pumps except for a 1983 USDA study [Refs. 1,12]. This involved laboratory testing with a permanent magnet three-phase 9 kw alternator designed for a windmill feeding a centrifugal pump. The instrumentation used was more complete and accurate than that available for the field tests reported here and the permanent magnet alternator restricted motor voltage control. Nevertheless, the investigators found that "standard three-phase, AC induction motors will pump water when operating at 30 hz and 85 volts" when the motors were rated at 230 volts and 60 hz. Their work characterized motor power output, efficiency and temperature rise in a complete manner not possible in the tests reported here due to inaccessibility of the motor shafts in commercial pumps.

Direct water pumping and heating is also possible using wind energy. The use of wind-driven centrifugal pumps for water heating has been explored [Ref. 3] and this method of heating could be compared with a heat pump driven by a stand-alone electric windmill as reported in this study. Models of pump behavior are widely available [Ref. 4] and the behavior of wind-driven pumps is described in a recent book [Ref. 5].

The control of a separately-excited wind driven alternator has been addressed by a number of manufacturers of windmills. Some recent innovative work is described in [Ref. 13].

The behavior of single-phase submersible pumps was not referenced in these papers and neither was work on single-phase heat pumps. Nevertheless, the insights presented in the referenced papers aided the investigators in this study and verified several of the required controller properties listed in Section VIII.

III. CHOICE OF TEST LOADS

A generic listing of electric farm equipment is shown in Table 1. Most devices are rated at 115 or 230 volt single-phase 60 Hz since three phase service is not available on most farms or if available, is more expensive than single-phase service. Multiple single-phase farm services totaling 800 amps at 240 volts are said to exist. The National Rural Electric Cooperative Association (1800 Massachusetts Avenue, Washington, DC) is one source of agricultural load information and the USDA at Ames, IA is another. A study sponsored by NRECA [Ref. 6] reports peak demand for a 120 cow dairy farm as 29 KW with about 1/2 of this load due to electric motors. The brief survey done for this report found most motors at 230 volts, single phase with nameplate horsepower mostly under 7.5 hp but with some motors purportedly as high as 50 hp. The majority of motors are fractional or 1 to 5 hp motors with caged rotors.

Many materials handling applications have high starting loads and are used intermittently such as conveyers and loading and unloading of biomass materials.

Ventilation applications (fractional to 2 hp) often pump a fixed air-flow volumetric rate against a small positive pressure for air supply and temperature control of animal housing (hogs, poultry). Grain drying and aeration operations require sufficient pressure to penetrate piled grains. Some materials, such as chopped silage, is moved by air flow so velocity in such systems must be maintained to silo heights.

Water extraction, circulation and heating is done on every farm and since storage is possible in ponds and tanks, can be done intermittently when alternative power is available.

Refrigeration is necessary in dairy operations and poses special problems due to high starting loads and to the sealed motor-compressor configurations usually used. Heating is used for crop drying and animal housing in cold climates.

The investigators chose for testing and analysis three of these loads which they believe are critical to many agricultural operations. These are:

- The extraction of water from deep wells.
- The circulation of water from storage reservoirs for animal watering and crop irrigation.
- The heating of air by a heat pump since it involves both air circulation across the condensor and evaporator and a hermetic motor-compressor package as used in refrigeration. Attempts were made to borrow a milk cooler to represent a hermetic cooling load but only an air-to-air heat pump-air conditioner could be obtained and tested.

FEED PREPARATION —

burr mills
hammer mills
roller mills
roughage shredder
feed blenders
feed meterer
feed mills, automatic
feed mill equipment and accessories
corn shellers
seed and grain cleaners

FEED HANDLING AND CONVEYING EQUIP. —

farm scales
silo unloading devices
bunk feeders
feed conveying equipment
bucket type elevators
hay mow conveyors
sweep un-loader
grain bin un-loader devices
wagon and truck un-loading devices
wagon loading device
auger or screw conveyors
elevators and/or conveyors
fruit and vegetable equipment

CROP AND GRAIN DRYERS —

batch dryers
continuous type dryers
heated air units
supplemental heat units
aeration fans
crop moisture meters
crop drying accessories, bins
grain probe thermometer

ENVIRONMENTAL CONTROLS —

fans, ventilating
walk-in coolers
insect destroyers
soil pasteurizer
insulating glass
switches
thermostats

EMERGENCY GENERATING EQUIPMENT —

electric generating sets (gas)
electric generating sets (diesel)
electric generating sets (tractor driven)
motors and accessories

***ELECTRIC HEATING* —**

electric heating
heating cable
temperature controls
in-line heaters
crop drying equipment
environmental control

WATER SYSTEMS —

pumps (shallow well)
pumps (deep well)
pumps (portable)
hot water heaters
water softener systems
water purification
water systems accessories
irrigation system equipment

MANURE DISPOSAL —

barn cleaners or gutter cleaners
liquid manure disposal systems

DAIRY EQUIPMENT —

milking machine units
pipeline milking units
bulk coolers
walk-in coolers
churns
pasteurizer
heat recovery unit
dairy ventilation
heating units
hot water heaters
dehorners and branders
clippers
dairy housing
cattle cleaner

POULTRY EQUIPMENT —

incubators
brooders
poultry feeders
poultry waterers
egg cleaning and handling equipment
laying nests
poultry ventilating equipment
walk-in coolers — other coolers
fountain medicator
debeaker
scalder
time controls
poultry housing

FEEDLOT EQUIPMENT — CATTLE, SHEEP, SWINE EQUIPMENT AND HOUSING

self feeders
waterers
ventilation equipment
water level control unit
heating units (floor heaters)
heating units (tank deicer)
de-horners and branders
clippers
electric fence controllers
gates
farm scales

SHOP EQUIPMENT —

air compressors
welders
soldering tools
power tools
cement mixers
battery chargers
steam cleaners
heating units
engine starting units
incinerators

Table 1 Farm Electrical Loads

The additional requirements included single-phase 60 Hz units in common use (mass-produced) with horsepower under 2 [1.5 kw] so that the 5 KVA power source used for the tests could start them under load, and permanent split capacitor windings so there were no centrifugal-switches to affect low speed and thus low frequency operation. This is a significant restriction since many motors use internal centrifugal starting switches to disconnect a starting winding at about 75% of normal speed.

Table 2 summarizes the specifications of the tested loads. The investigators thank the manufacturers of these devices for providing the further design information necessary for computer simulation of the behavior of their products.

Since the project was planned to evaluate feasibility of off-nominal operation in agricultural applications, the devices were field tested under conditions that were intended to represent typical applications. While the feasibility of operating other farm loads with wind power could be tested, the investigators believe that water pumping operations are necessary for all farming operations. Heat pumping to and from air is less critical for non-dairy operations but is of importance for space conditioning for residences as well as for farm building and so was included.

The submersible pump was suspended in a steel well casing inside a well-house with the plastic output pipe feeding a well-head flow meter and pressure gage before discharging thru a gate valve into a long plastic pipe. This setup is diagrammed in Fig. 1 and a photo shown in Fig. 2.

The circulating pump, a plastic self-priming rotor inside a cast housing, drew water from a farm pond thru a foot valve and short pipe and its output flow fed thru the same flow-meter, pressure gage and valve as above before entering a plastic pipe 110 meters long which returned the flow to the pond at a small head. The set up is illustrated in Fig. 2 and 3. The initial test used a stock tank and a shorter pipe before the pond was used.

The air conditioner-heat pump was a typical 1 1/2 ton residential unit with an exterior enclosure containing controls, hermetic motor-compressor (the latter with plug pistons), shaded-pole fan and outside heat exchanger. Two standard-lengths of precharged refrigerant lines fed the inside heat exchanger (baffled "A" coil). This coil divided a two-chamber plywood "furnace" with a squirrel-cage fan mounted at the bottom. The fan forced air upward thru the "A" coil, the upper plenum and out thru an opening 30% larger than the fan inlet area. The "furnace" (see Fig. 4) was instrumented with thermistors and draft gages. The set-up is illustrated in Figs. 5 and 6. This unit was loaned to the investigators by its manufacturer. Without this loan, the project could not have been completed.

Property	Submersible Pump	Circulation Pump	Heat Pump	Outdoor Fan Motor	Furnace Fan Motor	Variable Supply Alternator
Manufacturer	F.E. Myers Co. Ashland, OH 44805	F.E. Myers Co. Ashland, OH 44805	Addison Products Inc. Addison, MI 49220		Dayton Elect. Mfg. Co. Chicago IL 60098	Miller Elect. Mfg. Co. Appleton, WI 54912
Model Number	J10-18	QP10 with B828 motor	QH818		4C584	AEAD-200LE
Rated Freq. Hz	60	60	60		60	60 (100)
Rated Voltage RMS	230	230	230/208		115	240
Rated Amperes RMS	7.9	7.2	9.3/10.0 w/o fan (1.8)		8.9	5 KVA
Locked Rotor Amps	34	34	48.4	4. 4		44 (short circuit)
Run-start Capacitance	25 uf	25 uf	25 uf		shaded pole	
Rated horse-power	1	1		1/4	1/4	16.5 of gas engine prime mover
Rated speed rpm	3430	3450		1075	1050	1800 (3000)
Rated Pump Efficiency	51.8% @ 16 gpm	63.8% @ 40.5 gpm				
Motor Service Factor		1.4 (100% duty cycle 40° C)				100% duty cycle
Rated volumetric flow (near actual operating conditions)	22.5 gpm @ 115 feet total head	19.2 gpm		2670 cfm	1320 fcm	
Rated Power Output			19,300 BTU/hr @ 47° heating 17,800 BTU/hr @ 47°F cooling			
Rated Motor Input	1.22 KW		2.17 KW for above			
Load During Tests	100 ft 1 inch I D pipe to instrument manifold plus 150 ft outlet pipe	20 ft. 1 1/4"D inlet pipe to manifold + 25 ft. 1 1/4"D pipe to 300 ft 1"D pipe	Ambient air 59 - 71 °F			

Table 2 - Specifications and Properties of Tested Loads and Source

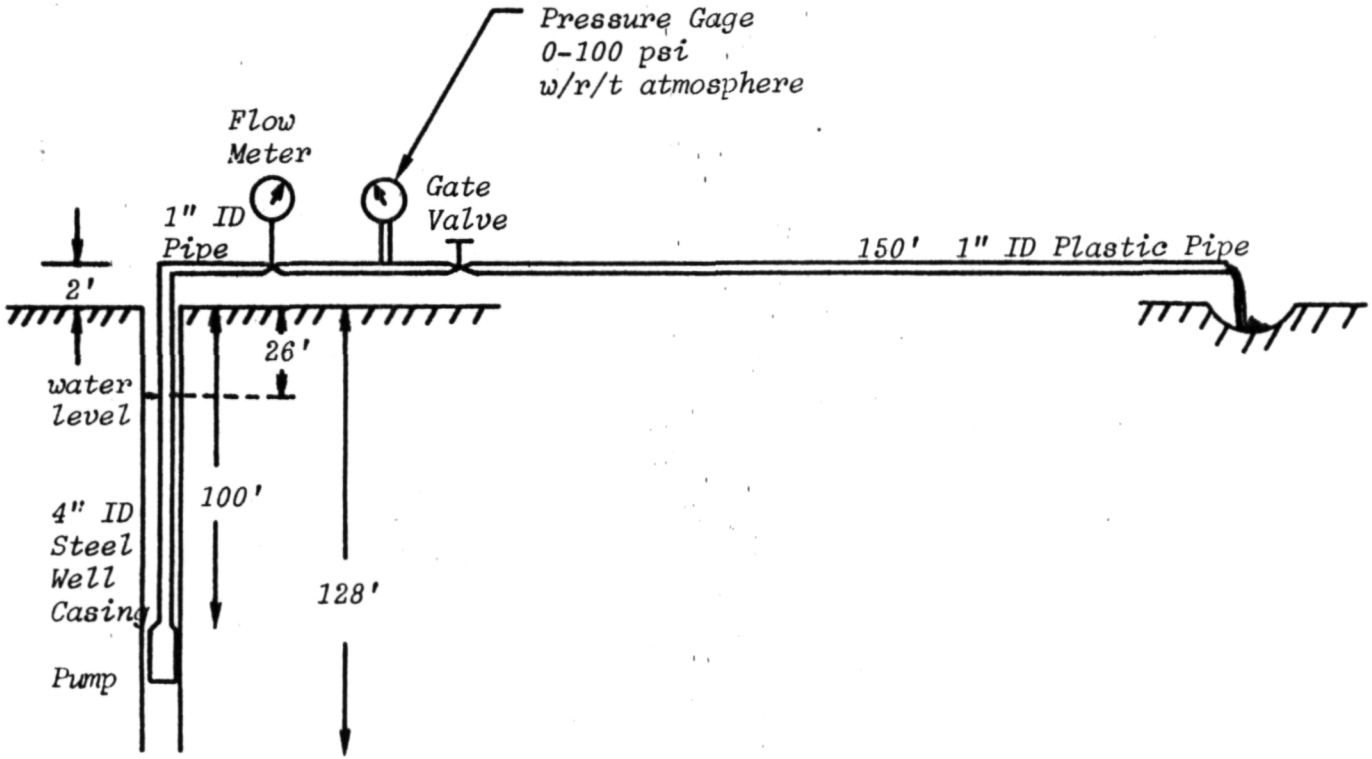

Figure 1

Schematic of Submersible Pump Test

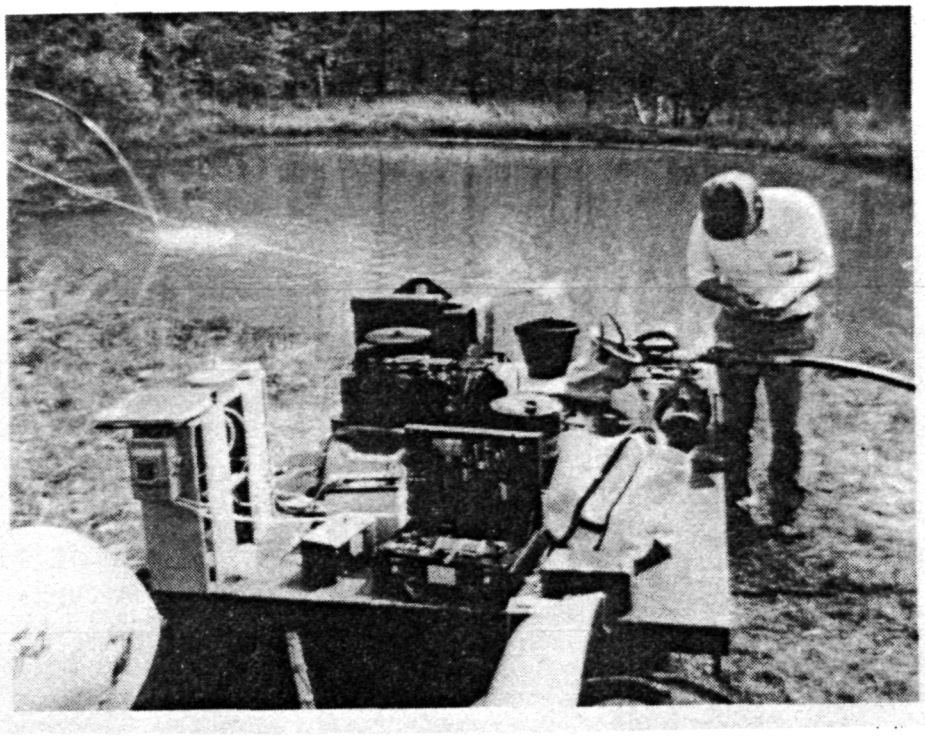

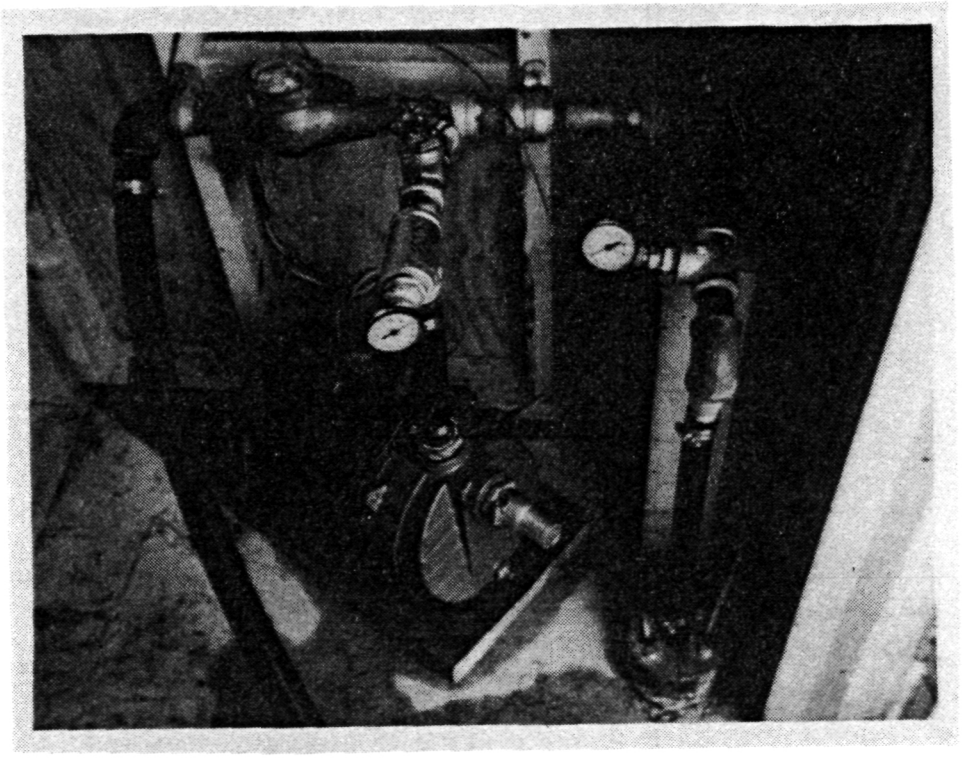

Figure 2

Photos of Water Pump Tests

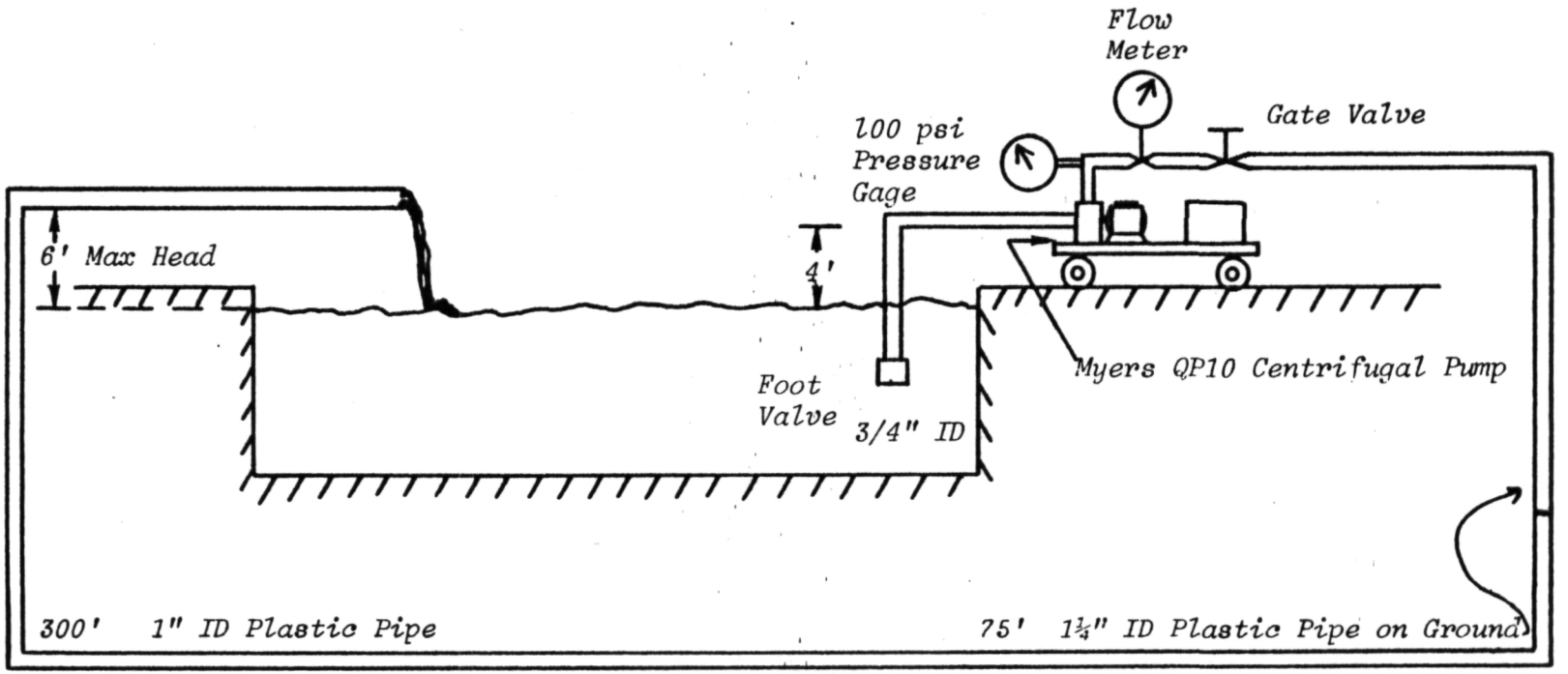

Figure 3

Schematic of Circulating Pump Test

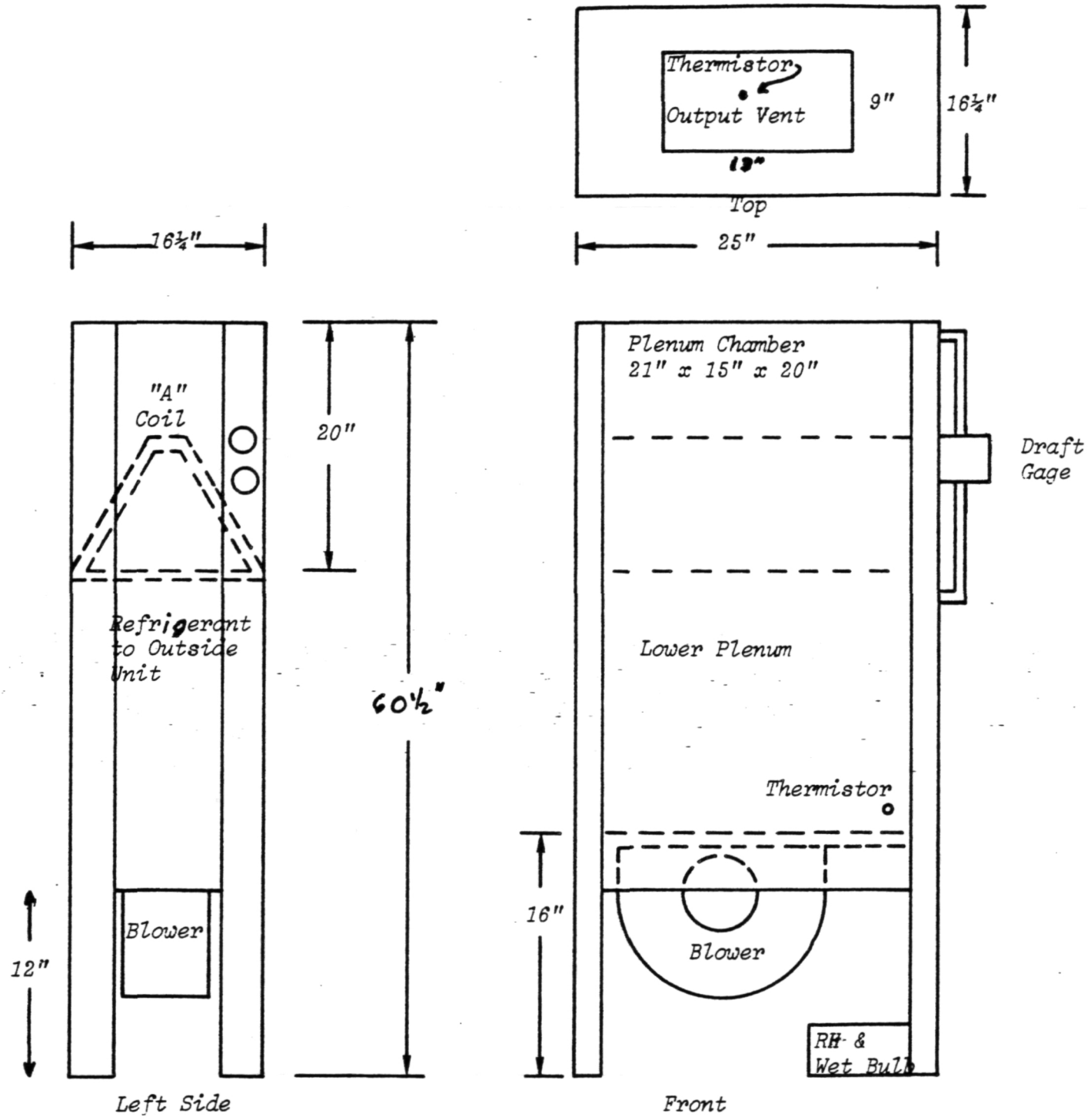

Mat'ls: 2" x 4" Legs & 1/2" Plywood for Remainder

Figure 4

Drawing of Heat Pump Furnace

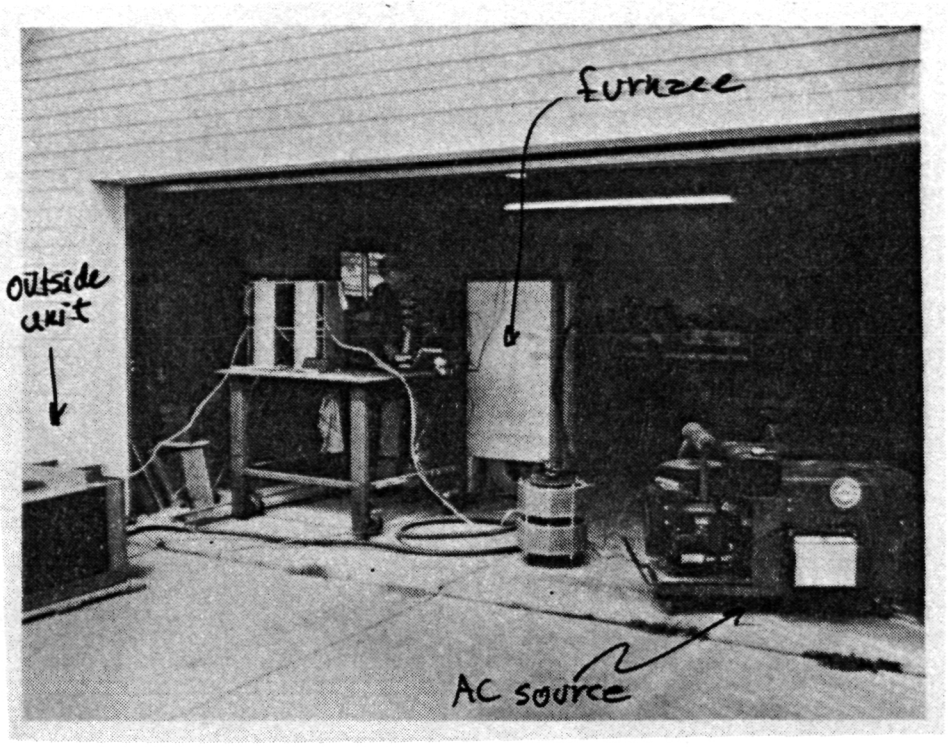

Figure 5

Photo of Heat Pump Test

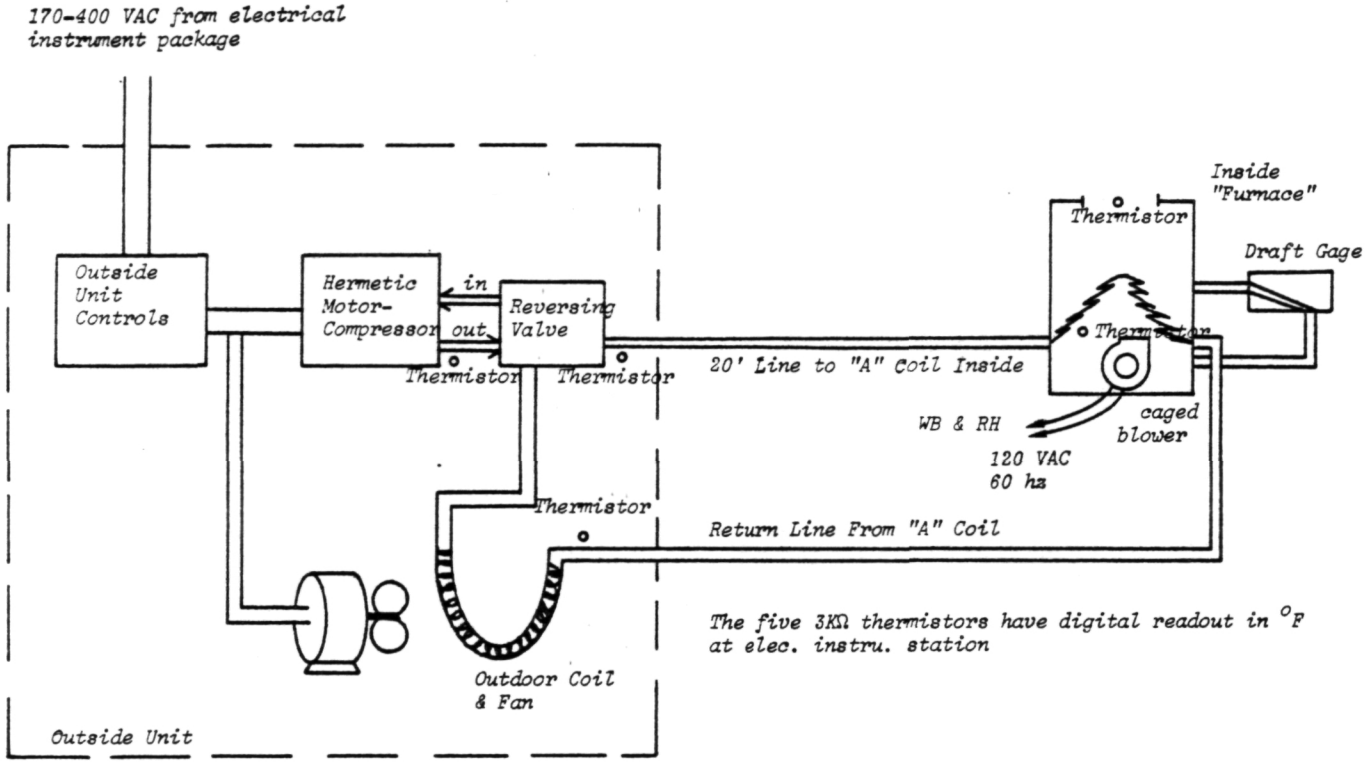

Figure 6

Schematic of Heat Pump Test

IV. MEASUREMENT TECHNIQUES, LIMITATIONS AND DATA REDUCTION

1) Instruments:

A sophisticated computer-based instrumentation system for this project would have absorbed the entire budget. Because the problem was simplified to determination of the steady-state operating envelope including power input and output variables, it was possible to use classic moving-pointer instruments and inexpensive field-grade transducers ordinarily used for commercial applications. The electrical input measurements were made with nearly identical setups for all three applications. Moving iron meters were used for voltage and current and a moving coil meter for power. Voltage and current readings were occasionally checked with a digital volt meter and clamp-on ammeters while frequency was measured with a digital meter and checked with an analog-output frequency to voltage hybrid integrated circuit package. A digital tachometer was used to verify the generator frequency measurements and to measure shaft speed on the furnace fan--the only load with an exposed shaft. Water flow was measured with a conventional commercial watermeter with a pulsed electrical output. Water pressure was read from a commercial Bourden-tube gage calibrated in psi. The flowmeter was checked by timing the filling of a 5 gallon can. The pressure measurements were not redundant--an unfortunate omission because pressure measurements are used to calculate pump power output and so should be double-checked.. For the heat pump test, temperatures were measured by thermistors with a digital readout and checked by a thermocouple--which was used with a wet sponge for wetbulb readings. Relative humidity was measured with a cheap "hardware store" gage. Static pressure in the "furnace" was measured with an inclined draft gage and roughly checked with a water-filled U-shaped manometer tube. Air velocity was measured with a mechanical pickup tube and meter. Load current or voltage waveforms were observed via a wideband toroidal current transformer or a toroidal potential transformer into a battery-powered oscilloscope. An extra set of thermistors was used to record the transient behavior of the heat pump piping temperatures to estimate time constants in the refrigerant loop. No flow or pressure transducers were available for monitoring the refrigerant loop. Power for the instruments that needed it in the water pumping tests out in the field was provided by a vibrator inverter of indeterminate age but impeccable reliability.

The test setups are diagrammed and photographed in Figs. 1 thru 8. The instruments and transducers are listed in Table 3.

2) Test protocol:

After the test setup was checked, the gasoline-powered welding generator was started and allowed several minutes warmup time. This generator was chosen because it will operate over a wide speed, and thus frequency, range without damage to its windings and because its exciter circuit allowed for considerable output voltage variation. However, the voltage variation was not

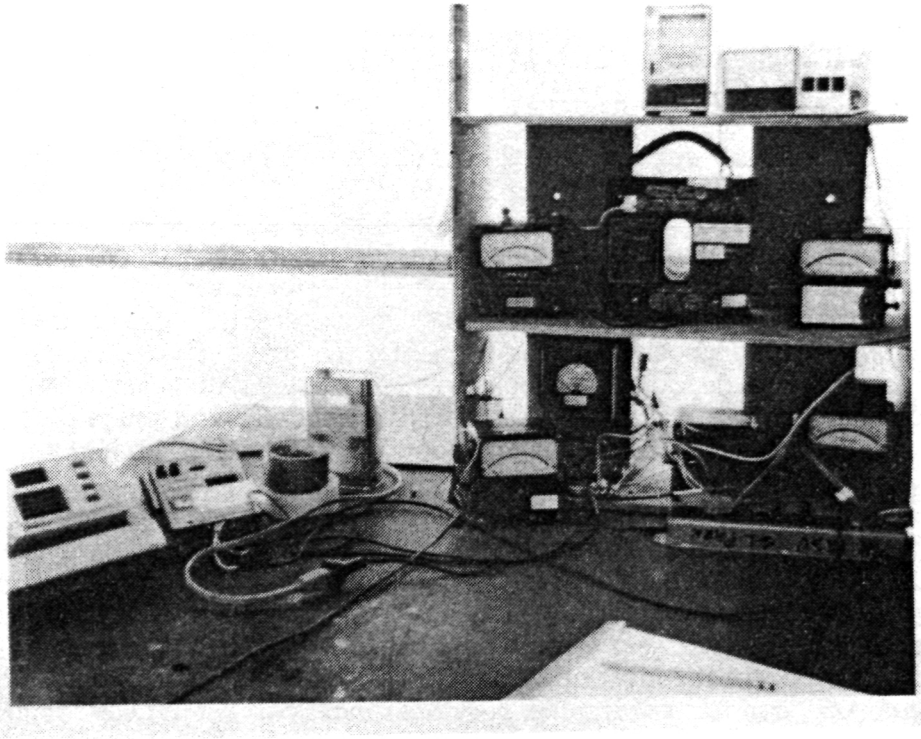

Figure 7

Instruments

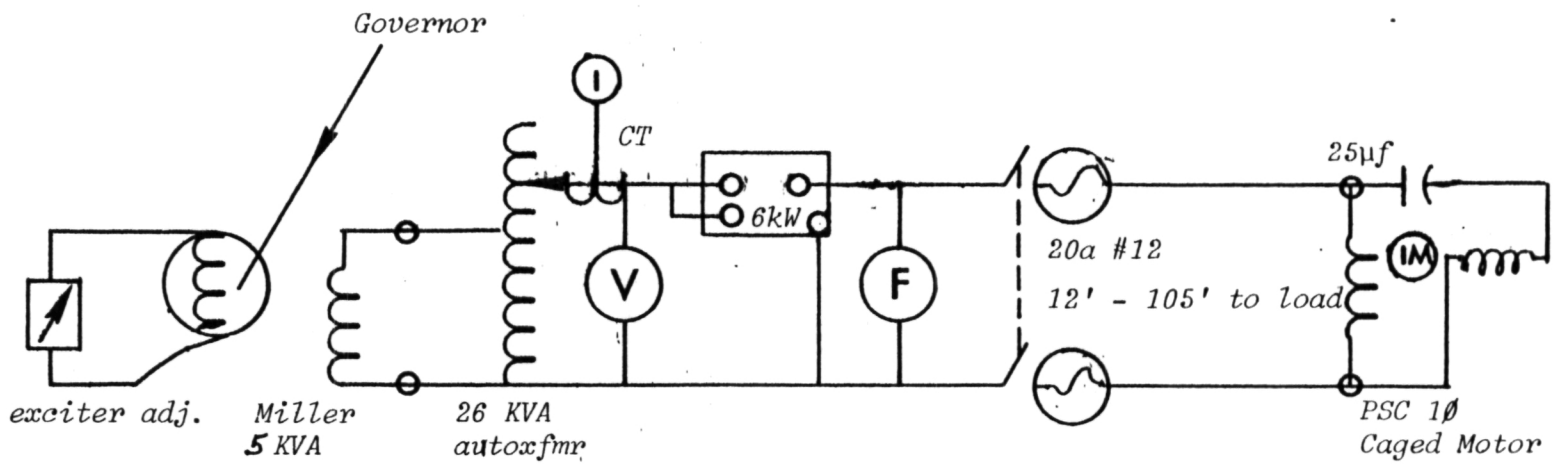

Figure 8

Schematic of Electrical Measurements

Instrument	Variable Measured	Type of Readout	Range(s) Used	Model #	Frequency range hz
Moving Iron Voltmeter	Pump Voltage	Mirrored Scale	0-300 (0-750)	Western 433	25-500 Hz
Current Transformer	Pump Current		5:1 & 10:1	Esterline-Angus Universal	25-125 Hz
Moving Coil Wattmeter	Pump Power	Mirrored Scale	0-3,000 0-6,000	Weston	
Multipurpose DVM	Check Voltage & Frequency	4 1/2 digits	0-750 volts 12-200 hz	Fluke 8060A	20-10 khz
Moving Iron Ammeter	Pump Current via CT	Mirrored Scale	0-2.5 0-5.0	Weston 433	25-500
Analog Frequency Meter	Frequency	Analog	0-200	Custom-based on AD451 IC	0-200
Clamp-on Ammeter	Check Current	Analog	0-30	Dayton 4 X 090	60
Current transformer	waveform of current	oscilloscope		Ion Physics CM-10-L	$10'-10^6$ Hz
Tachometer	supply frequency	5 digits	0-5000 rpm	Extech 461891	+ 1 rpm accuracy
Potential transformer	voltage waveform	oscilloscope	240 to 12 volts	Instru. Xfmr. Model 190	25-1000 hz
Flow Meter	analog dial & elect. counter	elect. counter	3-50 gpm	Master Meter MM5-01	
Pressure gages	water pressure	analog dial	0-100 psi		
Draft gage	air pressure	oil in inclined tube	0-1 in H_2O		
Manometer	check air pressure	U tube on inch scale	0-1 in H_2O		
Thermistor thermometer	temperature	2 switched 2 digit channels	$0-99^oF$	Heliotrope	3KΩ
Thermistor thermometer	temperature	2 switched 3 1/2 digit channels	$0-300^o$	Heliotrope Delta T	3KΩ
Thermocouple	Wet bulb or motor temp	Analog	$0-400^o$	Pyro Serve Mini J	
Draft gage	air velocity	analog	0-3000 fpm	Velometer	

Table 3

Instruments Used in Tests

as wide as the investigators desired and was increased for the heat pump tests by two 13 kva autotransformers operated in parallel. Furthermore, the generator governor was modified to allow steady-state operation over a range of speeds corresponding to 40 to 100 Hz.

With the generator warmed and operating at 60 hz and 230 volts, the load was switched on thru a fused switch and allowed to stabilize.. This took about 15 minutes for the heat pump but only a few minutes for the water pumps. After several measurements at nominal conditions, the generator throttle, field control, or autotransformer was varied to obtain a new test condition. The test conditions obtained and the time are noted in the data sheets reproduced in Appendix A from transcription of the rough field notes of the principal investigator. At the edges of the operating envelope, operation was unstable and the load motors either stalled due to inadequate torque, the water pumps cavitated, or the motors took so much input power that the run was terminated after or during the taking of readings. Motor overheating was noted only once when the heat pump motor thermal cutout opened and stayed open until the hermetic container was cooled. No motor winding temperatures were observed due to inaccessibility of the windings. After any shutdown, several minutes passed before a restart was attempted. For the heat pump, a longer interval was needed for the refrigerant pressures to equalize.

Approximately 170 sets of readings were taken during the successful tests over a period of several months and they all are included in Appendix A. The test site climatic conditions were moderate for the circulating and heat pump tests but below freezing for the submersible pump test which affected only the investigators and the instruments because the submersed pump was near 10°C.

3) Test limitations:

Inspection of the data sheets and the previous paragraphs suggest several limitations of the data—which the investigators believe do not change the conclusions of the study. However, if the study was to be repeated or extended, they should be considered in future test planning.

- For several heat pump runs at high frequency, the measured real power slightly exceeded the calculated apparent power—which is physically impossible. Wattmeter error is suspected since the current and voltmeters were rated from 25 to 500 Hz while the wattmeter is not.

- The digital readout for furnace input and output temperatures yields integral numbers so temperature differences across the "A" coil could be in error by as much as 7% with a corresponding error in heat power output.

- The flowmeter measurements were timed with a watch and small errors are likely.

- The load voltage was measured at the instrument package, not at the motor terminals at the end of 3 to 30 meters of #8 or #12 wire. This error might be as much as 2%.

- The generator governor could not always hold the frequency steady so the frequency regulation had a total variation (peak to peak) of one Hz.

- The pressure drop across the flow meter was estimated from the manufacturers data and not measured. Similarly, the pressure drop across the foot valves and the gate valve and the pipe couplings were estimated—not measured. This causes errors in the load characterization.

- The pressure gage had no negative pressure calibration marks so the circulating pump suction was estimated. This is likely to cause pump power output errors as much as 10%.

In spite of these errors, the investigators found the data set in general to be consistent and relatively close to values predicted by the computer simulation.

4) Test data reduction:

Calculations using test data were done for two reasons. The first was to describe the pump electrical input behavior in terms of input kva (apparent power) and power factor as well as pump output in kW. The latter required complex calculations and corrections since the mechanical outputs of the submersible and heat pumps were not directly available for measurement. The other reason was to model the pump loads so they could be BBincluded in the computer simulation models to allow comparison between predicted and measured performance. The results of the data calculations are entered in the columns marked by an asterisk (*) in the data sheets which are in Appendix A. The investigators regret the use of English units but their instruments were so calibrated and excessive conversions increase the possibility of error. However, the input and final output variables are presented in SI units.

The data reduction for the electrical input variables required few assumptions. The magnitude of the apparent power is just the pump input amperes times the pump input voltage. The burden of the electrical instruments was 5 VA or less so no loading corrections were necessary. The ratio of measured real power from the wattmeter to the calculated apparent power gave the power factor of the pump under test for the input conditions observed.

The pump power output calculations used data from less accurate gages and required more assumptions and are thus less accurate. However, since the same assumptions and resultant corrections were used for all runs of each of the three loads, the pump behavior is fairly characterized by comparing the power output behavior at nominal or rated conditions with the output under significant deviations from those rated or nominal conditions.

Power output corrections for submersible pump:

Since power is force times velocity or pressure times volumetric flow, and since the instruments were calibrated in English units, the S.I. formula

$$\text{Power} = \text{Pressure}\left(\frac{N}{m^2}\right) \times \text{Flow}\left(\frac{m^3}{sec}\right) \text{watts}$$

is converted to

$$\text{Power} = 0.4350 \times \text{GPM} \times \text{PSI watts}$$

where GPM is flow in gallons per minute and PSI is total head in pounds per square inch—which are the units of the instruments and of the pump specifications. If pressure had been measured at the outlet pipe discharge, and converted to head, then total head in this equation would have been this pressure head plus the difference in altitude between input and output water levels. This was not done so the following corrections were used to estimate pump mechanical output from the measured data. In the submersible pump measurement configuration used, this formula yields power measured at the surface manifold where the pressure is measured after the flow transducer. Corrections are needed for the pressure drops caused by: the flow transducer; the submerged foot or inlet valve at the pump input; and the friction loss of the 100 feet of pipe between the submerged pump outlet and the manifold. The power needed to lift the water flow against gravity is also required to estimate the pump output at its outlet.

The power required to lift water against the gravity field is proportional to the net head times the volumetric flow. Since the net head (the difference in elevation between the water level in the well casing and the manifold at the surface) is about 7.93 m, the power required is

$$P_{lift} = 4.904 \times \text{GPM watts}$$

Although derived here from first principles, this formula yields the same results as Johnson [Ref. 5, p. 282]. The pressure drop correction due to friction from the 100 feet (30.48 m) of 1 inch ID (.0254 m) smooth plastic pipe first requires an estimate of the Reynolds number (R_e) of the pumped fluid. Across the range of measured flows (about 5 to 30 GPM), R_e ranges from 1.38×10^4 to 8.27×10^4.

The relation is, for water at 50°F (10°C),

$$R_e = 2758 \times \text{GPM}$$

Assuming that the plastic pipe is very smooth, the corresponding friction factors range for $f(R_e)$ of 0.027 to 0.018 [Ref. 7, p. 95]. The head loss Δh due to this friction is

$$\Delta h = f \times \left(\frac{\ell}{D}\right) \times \left(\frac{V^2}{2g}\right)$$

where ℓ/D is the length to diameter ratio of the pipe, g is the gravity constant, and V is the flow velocity. In the units of the instruments, this becomes for this test configuration

$$\Delta h = f(GPM) \times 3.109 \times (GPM)^2 \text{ feet}$$

Since the pressure loss and the head are related by the fluid density, the correction becomes

$$\Delta PSI = 1.347 \times f(GPM) \times (GPM)^2 \text{ pounds per square inch.}$$

Thus, for each flow measurement, the corresponding pressure drop due to friction can be found.

The pressure drop for the flow meter is given in the manufacturers data sheet and is included in Table 4. The pressure drop in the pump inlet valve is assumed equal to that of a half-opened gate valve of the same diameter or with K = 5.6 in the formula

$$\Delta h = H \frac{V^2}{2g}$$

In terms of pressure loss, this becomes

$$\Delta PSI_{\text{foot valve}} = 0.006288 \ (GPM)^2 \text{ pounds per square inch}$$

These pressure drops were added, converted to watts, and all corrections were added to give a total correction to measured surface output in watts as shown in Table 4. The corrections are plotted in Fig. 9 which was used to estimate the correction for each pump run and added to the measured surface power to get the estimate of pump power output shown in the data sheets and used to illustrate the measured behavior of the pump in Section V.

Power output from circulating pump:

There was no correction made for the output calculation of the circulating pump. The output formula used was

$$\text{Power} = 0.4350 \times GPM \times PSI \quad \text{watts}$$

as in the case for surface power for the submersible pump. The suction pressure calibration was poor so these readings likely induce more error for this load where the PSI reading should be the pressure rise across the pump since the input and output water elevation was the same.

Output calculations for the heat pump:

The thermal output power calculation from the furnace output vent driven by the outside compressor via the refrigerant loop and heat exchanger (the "A" coil) in the furnace requires several variables. They are the air mass flow (AMF), the temperature difference ΔT across the "A" coil, and the specific heat of the air flow thru the furnace. Again, the instruments and heat pump components used were calibrated or specified in English units so

GPM	$\Delta PSI_{friction}$	$\Delta PSI_{flow\ meter}$	ΔPSI_{inlet}	ΔPSI_{total}	Power equiv. watts	Power to lift watts	Total power correction watts
5	0.909	0	0.157	1.07	2.3	24.5	27
10	3.23	0	.629	3.86	16.8	49.04	66
15	6.67	1.1	1.415	9.19	60.0	73.56	134
20	11.04	2.25	2.515	15.81	137.5	98.08	236
25	16.0	3.5	3.93	24.43	265.7	122.6	388
30	21.82	5.66	5.66	32.38	422.56	147.12	570

Table 4 Submersible Pump Output Power Corrections

Figure 9

Power Output Corrections to Adjust Measured Surface Power to Submersible Pump Output

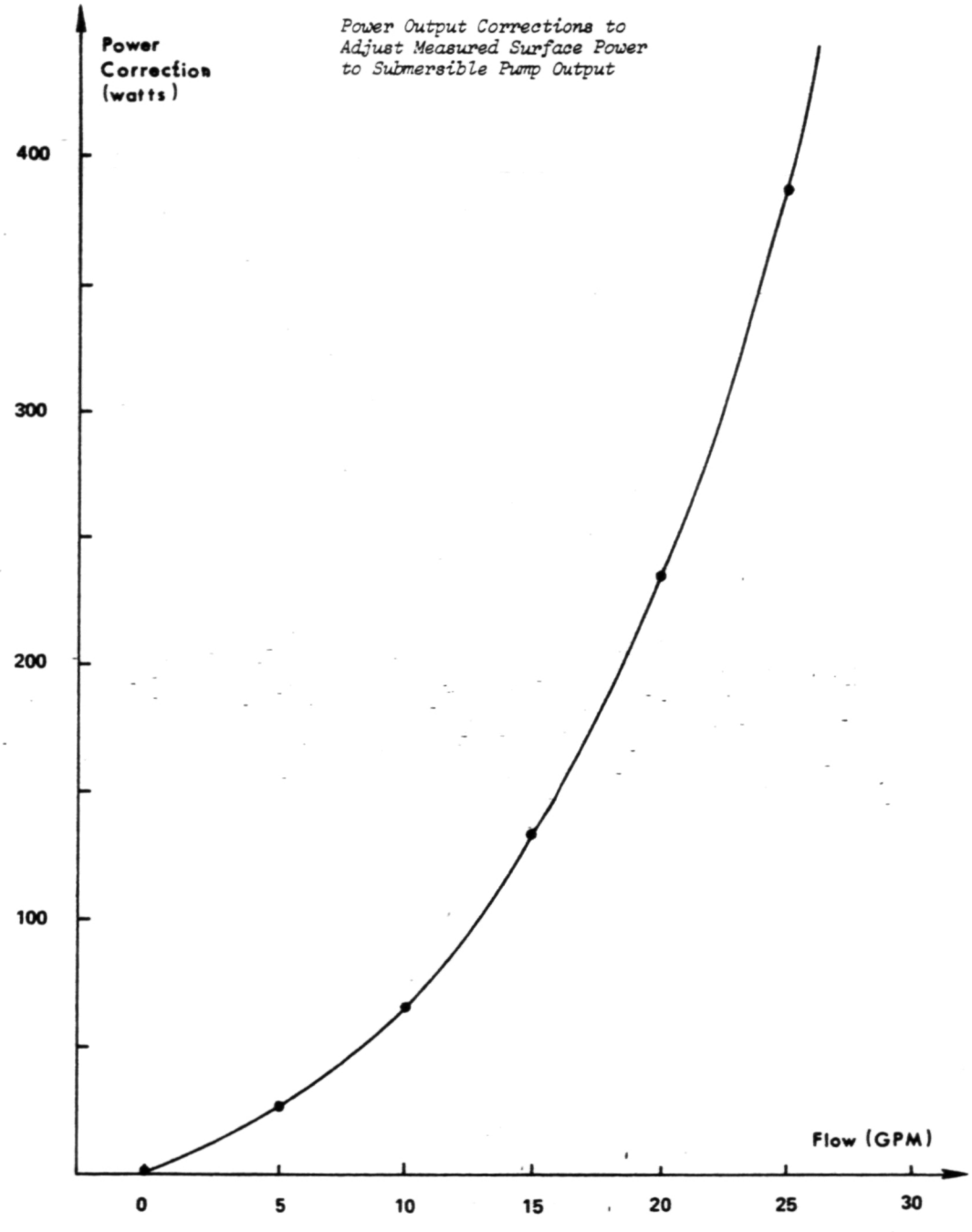

these were used for the intermediate calculations although the output was expressed in kilowatts.

The volumetric air flow is needed to find the air mass flow and the former was found from the furnace blower fan specifications and roughly checked by an air velocity profile taken at the exit vent to the furnace output plenum chamber. , The fan specifications (the Dayton fan is described in Table 2) give a flow of 1320 ft^3/min against a head of 0.6 inches of water with a fan motor current of 8.9 amperes at 115 volts 60 Hz AC and a fan shaft speed of 1050 rpm. On the first day of testing, the measured static pressure in the fan plenum was 0.61 inches of water at 1047 rpm with a measured draw of 8.9 amps at 117 volts and 60 Hz and with a measured power input of just under 600 watts. Interpolation of the fan catalog data suggests 1313 ft^3/min of flow. A few small leaks in the plywood furnace were taped before the second day of testing on May 21, 1985 and the pressure increased to 0.62 inches of water with 9 amps of current. The pressure increase suggests by interpolation a flow decrease to 1306 ft^3/min but the increased current and a slight increase in fan power input suggests more flow so 1313 was used. A crude check was made by measuring the air velocity profile at the furnace exhaust vent with a velocity gage. The measured profile peaked at 2200 ft/min at the exhaust vent center and decreased to 1900 to 2000 ft/min at a distance of 1/2 inch in from the edges of the vent. The flow velocity was fairly regular due to the diffusing effect of the "A" coil fins. The assumption of an average outlet velocity of 2000 ft/min over an outlet area of 8 by 12 inches yields a volumetric flow of

$$\frac{8 \times 12}{144} \times 2000 \text{ ft/min} = 1333 \text{ ft}^3\text{/min},$$

which checks the 1313 figure interpolated from the manufacturers data.

To get the air mass flow (AMF) from the volumetric flow, an estimate of air density is needed. Using the assumptions that the air was relatively dry (the relative humidity was under 50%) and behaves as an ideal gas, the air density was calculated as:

$$\text{Density} = \frac{\text{Pressure}}{\text{air gas constant} \times \text{absolute temperature}}$$

The plenum pressure was small (.02 psi) so the absolute pressure was 2120 pounds per square foot--close to atmospheric. In English units

$$\text{Density} = \frac{2120}{53.3\ [460 + T_{plenum}\ (^{o}F)]} \text{ pounds mass/ft}^3.$$

Since air mass flow is density times volumetric flow,

$$AMF = \frac{52.224 \times 10^3}{460 + T_{plenum}\ (^oF)} \text{ pounds mass per minute.}$$

Over the range of temperatures encountered in the input plenum, which was 59°F to 71°F, AMF ranged from 100.62 down to 98.35 pounds mass per minute. AMF is shown in the data sheets.

The thermal power output of the heat pump, either in the heating or cooling mode, is:

$$P_{out}\ (\text{thermal}) = AMF \times \text{specific heat} \times \text{temperature difference.}$$

The appropriate specific heat constant is that for dry air at constant pressure since the pressure change in the furnace is very small. The value is $C_p = 0.24$ BTU/lbm-°F so the output formula becomes:

$$P_{out}\ (\text{thermal}) = AMF \times C_p \times \Delta T(^oF) = 14.4 \times AMF \times \Delta T(^oF) \text{ BTU/hour,}$$

which is in the units that heat pump manufacturers conventionally use. When this BTU/hr figure is divided by 3413 BTU/hour, the power output is in units of kilowatts. When the power output in kW is divided by the electrical power input in kW, the resulting number is the coefficient of performance which is about 3 for the test conditions. The power output calculations at nominal conditions yielded power outputs close to the manufacturers specifications.

Heat pump in cooling mode:

In this mode, where only a few measurement runs were made, the furnace fan was connected to the variable source so the air flow thru the furnace was affected by the source. Over the frequency range of 50 to 70 Hz, the fan plenum pressure changed only about .1 inches of water or less than one part in 10^3 in absolute pressure so the air mass flow will change significantly only due to volumetric flow changes. If one assumes this flow change will be proportional to frequency only, then

$$\text{Air flow} = \text{Air flow (60 Hz)} \times \frac{\text{Fan frequency}}{60}$$

Two checks were made at 70 Hz to validate this assumption. The measured peak velocity out of the exhaust vent increased to 2500 ft/min from the 2200 peak value at 60 Hz. If the average flow increases as much, the correction 2500 is 1.14 while the frequency correction just described is 70/60 or 1.17.

2200

The second check used the increased pressure drop of 0.40 inches of water across the "A" coil at 70 Hz where it was 0.31 at 60 Hz. This suggests a correction factor of

$$\text{AMF (70 Hz)} = \text{AMF (60 Hz)} \times \left[\frac{\Delta P \text{ (70 Hz)}}{\Delta P \text{ (60 Hz)}}\right]^{1/2}$$

$$= \text{AMF (60 Hz)} \times \left[\frac{.40}{.31}\right]^{1/2} = \text{AMF (60)} \times 1.136$$

The square root is used since AMF is related to velocity (at constant density—already justified) and velocity change is proportional to the square root of pressure change from the energy equation for compressible flow. The checks are OK so the output power of the heat pump in cooling mode with furnace fan excited by the variable frequency source is

$$P_{out} \text{ (thermal)} = 14.4 \times AMF_c \times \Delta T(^{o}F) \text{ BTU/hour}$$

where AMF_c is AMF corrected by frequency ratio. The AMF_c and power output data obtained by the calculations described above are included in the data sheets (Appendix A).

V. EXPERIMENTAL RESULTS

Since data was available for about 170 test runs it would be easy to overload the reader with multiple presentations of data. Furthermore, the conventional method of presenting motor data [eg: Ref. 2], is to plot with motor shaft power output as independent variable--and the motor shafts were inaccessible for measurement. Thus, the investigators were forced to present the data in an unconventional manner and, after considerable deliberation, decided upon the "operating envelope" concept common in aircraft performance analysis. Here the range of variables for stable operation is presented with the suggestion that operation outside of this envelope is either unstable or unsafe. The usual variables for aircraft in level flight are speed and altitude while in this report, the investigators chose input voltage and frequency. In some plots, the power input and power output corresponding to each voltage-frequency data pair are included. A glance at the "envelope" is instructive as it suggests the range of input combinations at which the particular pump will operate. It is also possible to indicate the reason for unsuccessful operation at the edges of the envelope. The reader will notice that motor stall due to inadequate torque, in turn due to inadequate excitation voltage, is noted at the bottom of the envelope and cavitation and overload is often present at high frequencies. High voltages would be expected to also increase iron losses with resultant overheating. However, most runs were too short for overheating to appear and besides, winding temperatures were not measured.

It should be noted that the high voltage side of the envelopes are not completely explored since the excitation system of the source, even with the autotransformer is inadequate to provide voltages much beyond 50% of nominal. The other presentation technique used was a conventional plot of load power ratio (where nominal or rated is unity) as either voltage or frequency is varied while the other is held nearly constant. All of the measured data points come from the data sheets in Appendix A.

1) Experimental results for F.E. Myers J 10-18 submersible pump

In Fig. 10, a partial envelope of the submersible pump indicates that this pump will operate between 42 and 100 Hz and requires less voltage as the torque requirements decrease with pump speed (frequency). The power input and output numbers show that the overall efficiency decreases above 75 Hz when apparently cavitation begins. There are too many data points closely grouped to include the power numbers. Therefore, just the voltage and frequency pairs are plotted in Fig. 11. A stable condition means that the measured pump variables did not change significantly during that test. In Fig. 12, the submersible pump power ratio from nominal frequency is plotted for voltage within 3% of nominal 230 volts. A linear representation of this data indicates a change of pump power input of 2.2% for a 1% change in frequency. The increase in power with cccfrequency indicates that as windmill rotor speed increases during a gust, the load will also increase to moderate rotor acceleration.

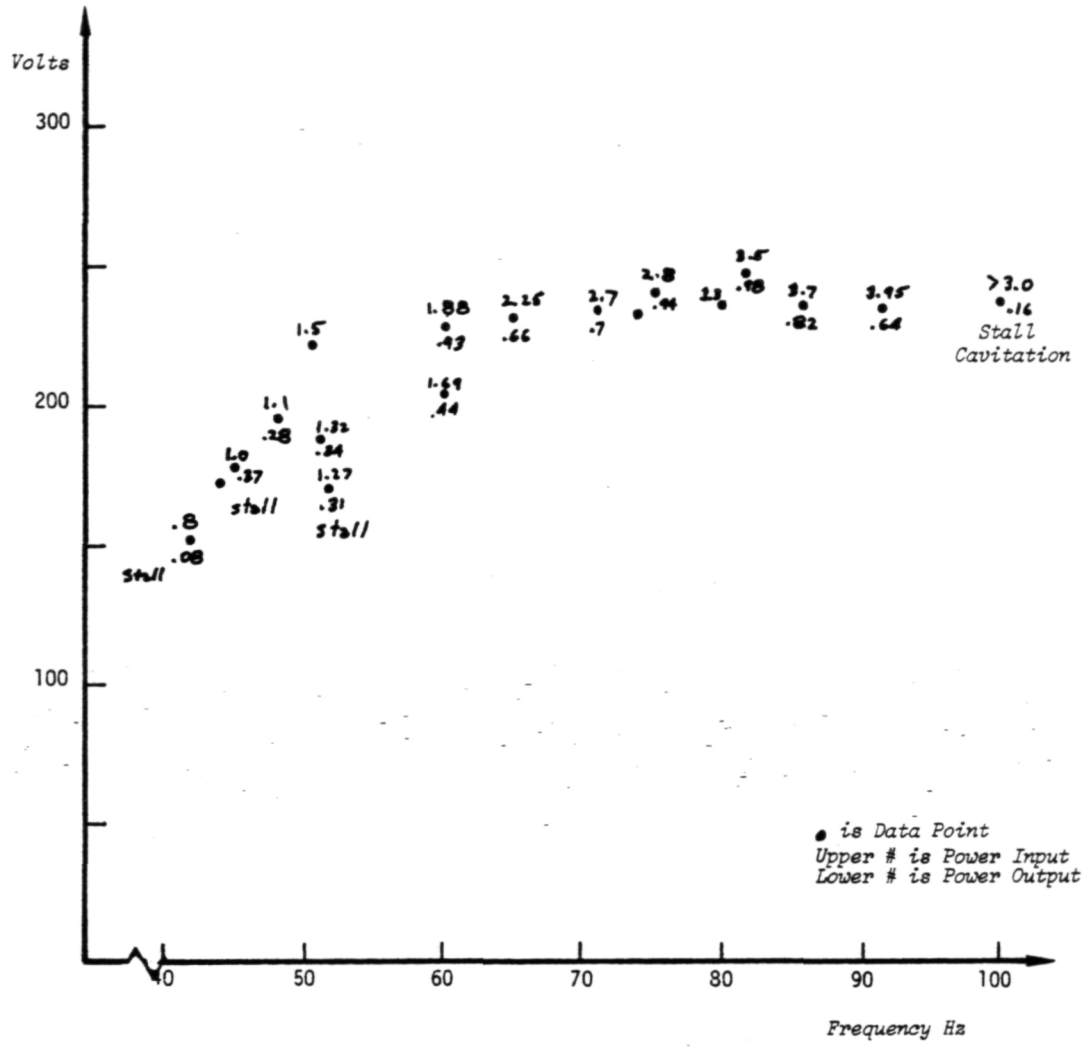

Figure 10

Measured Partial Operating Envelope of Submersible Pump Showing Input and Output Power

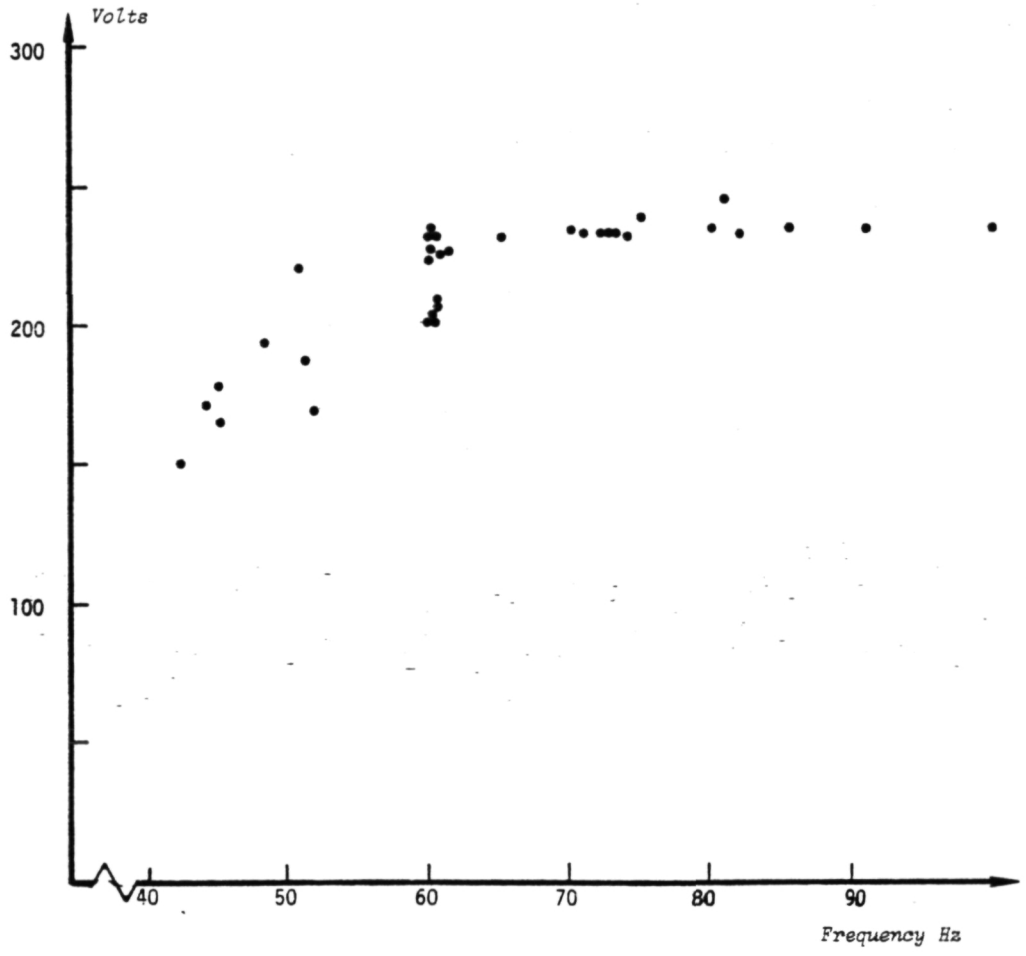

Figure 11

Measured Stable Voltage-Frequency Pairs for Submersible Pump

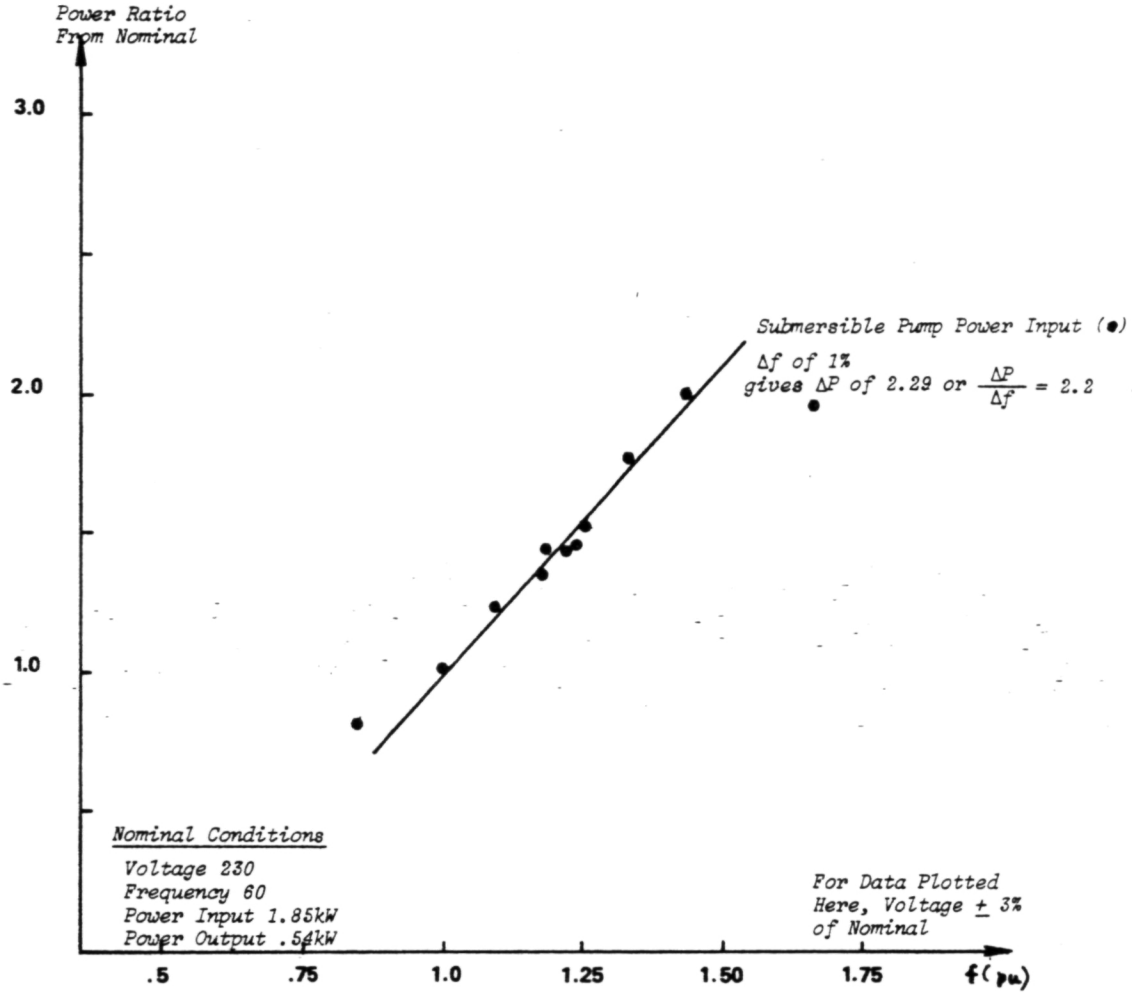

Figure 12

Variation in Submersible Pump Power as Frequency is Changed

2) Experimental results for F.E. Myers QP10 centrifugal circulating pump

The measured operating envelope for the circulating pump with long pipe load is shown in Fig. 13. The frequency range is less than the submersible pump—from 48 to 92 Hz but the stable voltage range is greater—from 94 to 275 volts. The same pump with a lesser load (pipe length about 1/2 of above, gate valve wide open and no inlet valve) has a higher output but operates over the same range indicating the range is dominated by motor characteristics. Not enough data points are available for a reasonable estimate of the operating envelope under this loading. The data available is shown in Fig. 14. The two figures indicate that the centrifugal pump can tolerate more voltage variation than the submersible pump but that stable operation at low frequencies is harder to maintain. Furthermore, this type of pump requires a foot valve at its suction pipe inlet to avoid loss of prime. The investigators suspect that maintaining prime (avoiding loss of suction) will be required for intermittent operation as provided by a windmill source. Fig. 15 illustrates the behavior of this pump as voltage is changed while the frequency is maintained within 1/2 Hz of 60. The pump power input is not sensitive to voltage changes so that 1% increase in voltage causes only a 0.4% increase in pump input power.

3) Experimental results for Addison QH818 heat pump

Unlike the water pumps, the heat pump was field tested under reasonable climatic conditions with a test setup capable of greater excursions in voltage and frequency and with greater redundancy in output measurements. Fig. 16 shows the measured stable operating points for the heat pump in heating and cooling modes. The addition of the autotransformer, not available for the water pump tests, allowed voltages to reach almost 400 volts at the higher frequencies and the pump operated without noticeable complaint down to 50 Hz before stalling around 47 Hz. The lowest voltage of operation is 175 volts which confirmed a test run by the Principal Investigator in June 1971 when 180 volts was the lower limit of stable operation for a Sears 14,000 BTU/hour air conditioner rated at 230 volts [Ref. 8, p. 29]. In that 1971 test, the compressor-motor power factor was close to unity at that voltage which is also true for the heat pump at low voltage. The 1971 tests were run only at 60 Hz. The Addison chief engineer warned that the compressor outlet temperature must remain under 260° F, to avoid lubrication problems, and the data indicates a maximum of 213°F which occured during a 90 Hz run. Fig. 17 shows a subset of the data with input and output numbers included. Note that the coefficient of performance approaches four near 50 Hz but drops toward two over 85 Hz. and at voltages over 320 where motor excitation and pumping losses increase. When the voltage decreases, the motor current increases so winding losses increase and high motor temperatures seem likely. This was verified by the opening of the thermal cutout in the motor winding which occurred after ten minutes of operation at low voltages. The motor was drawing (both the compressor motor and outside fan motor together) 13.1 amps (rated is 11 amps) when the cutout opened. Nevertheless, the heat pump will operate on a short-term basis over a range of voltage and frequency that surprised the investigators.

The variation in heat pump input and output power as frequency is varied is shown in Fig. 18. Note that the power output line is much flatter than the input line and the crossover is at 92% of rated frequency which support the

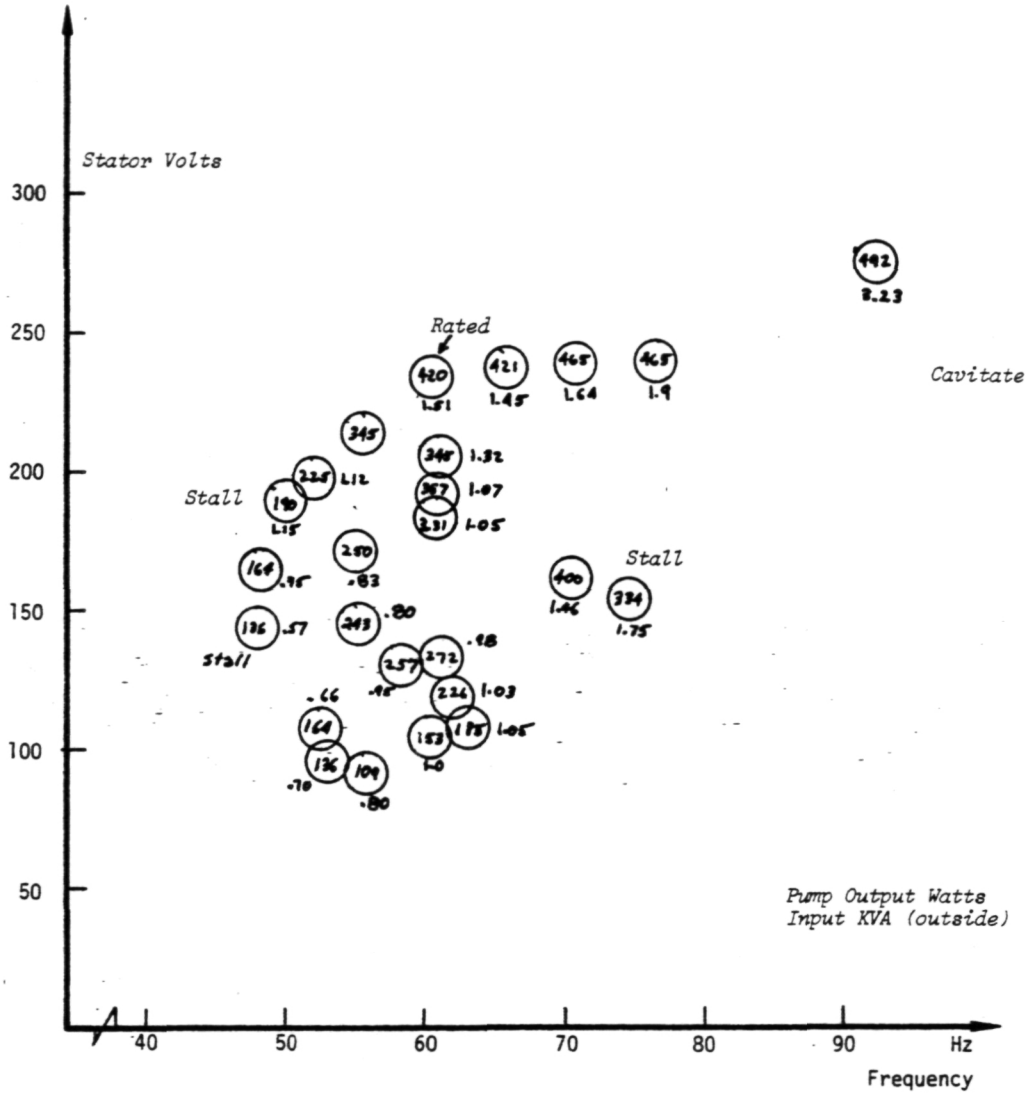

Figure 13

Measured Operating Envelope of Circulating Pump with Long Pipe Load

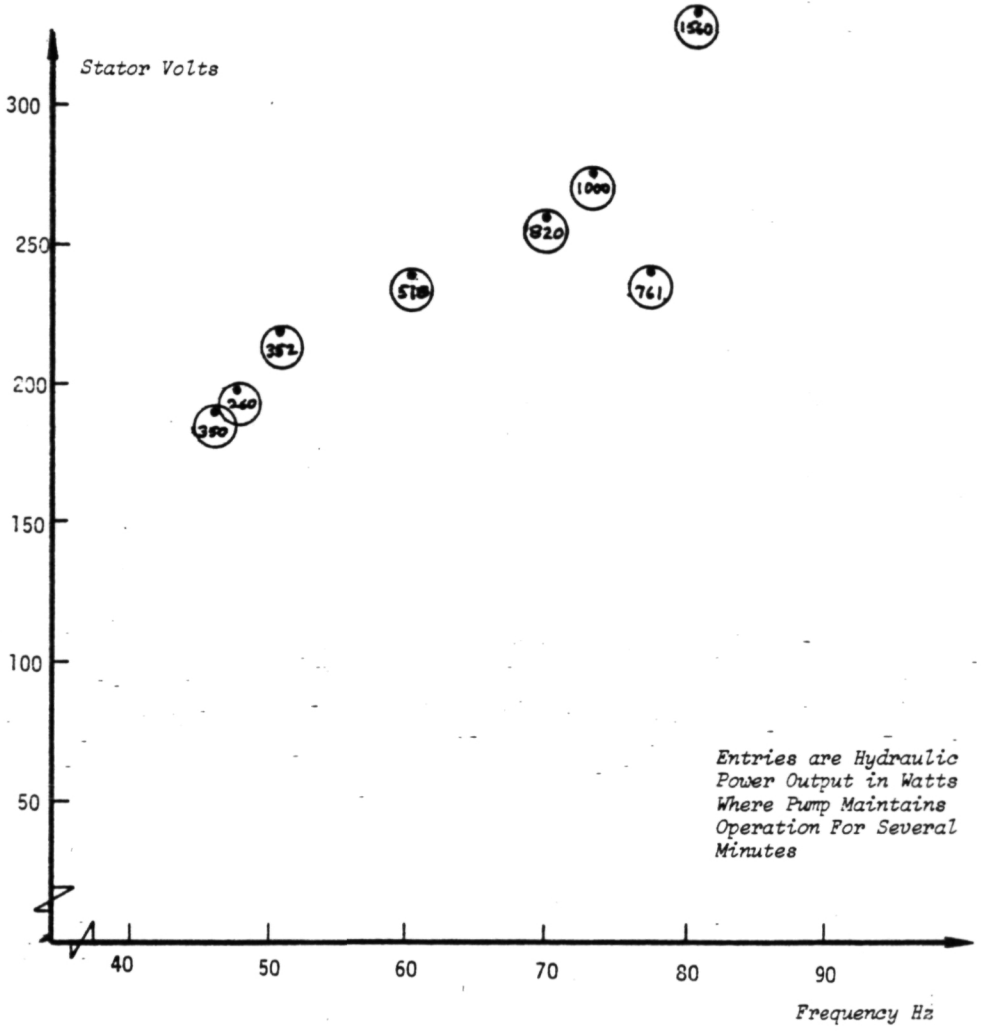

Figure 14

Measured Partial Envelope of Circulating Pump with Shorter Pipe Load

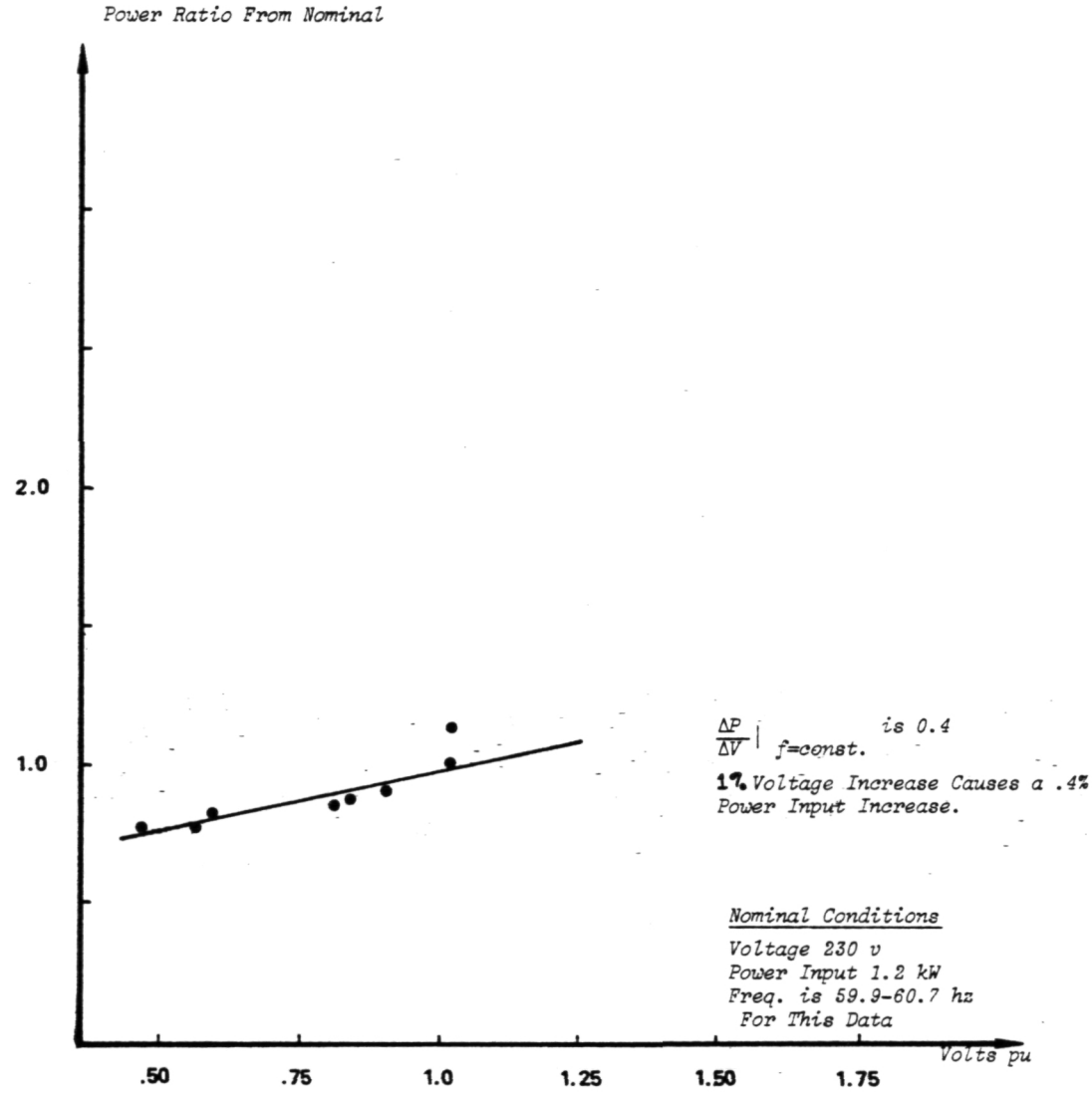

Figure 15

Variation of Circulating Pump Input Power as Voltage is Changed

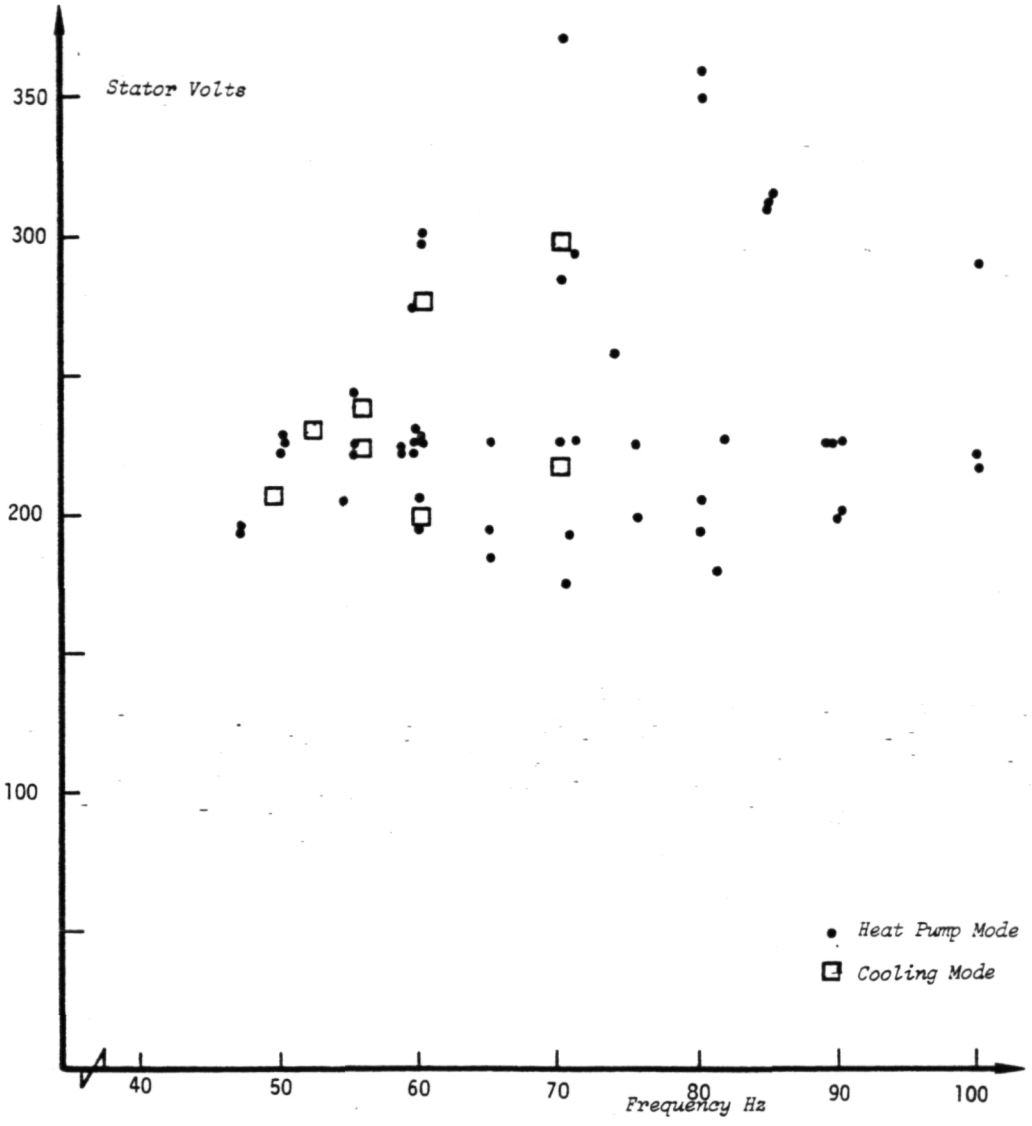

Figure 16

Measured Stable Voltage-Frequency Pairs for Heat Pump in Heating and Cooling Modes

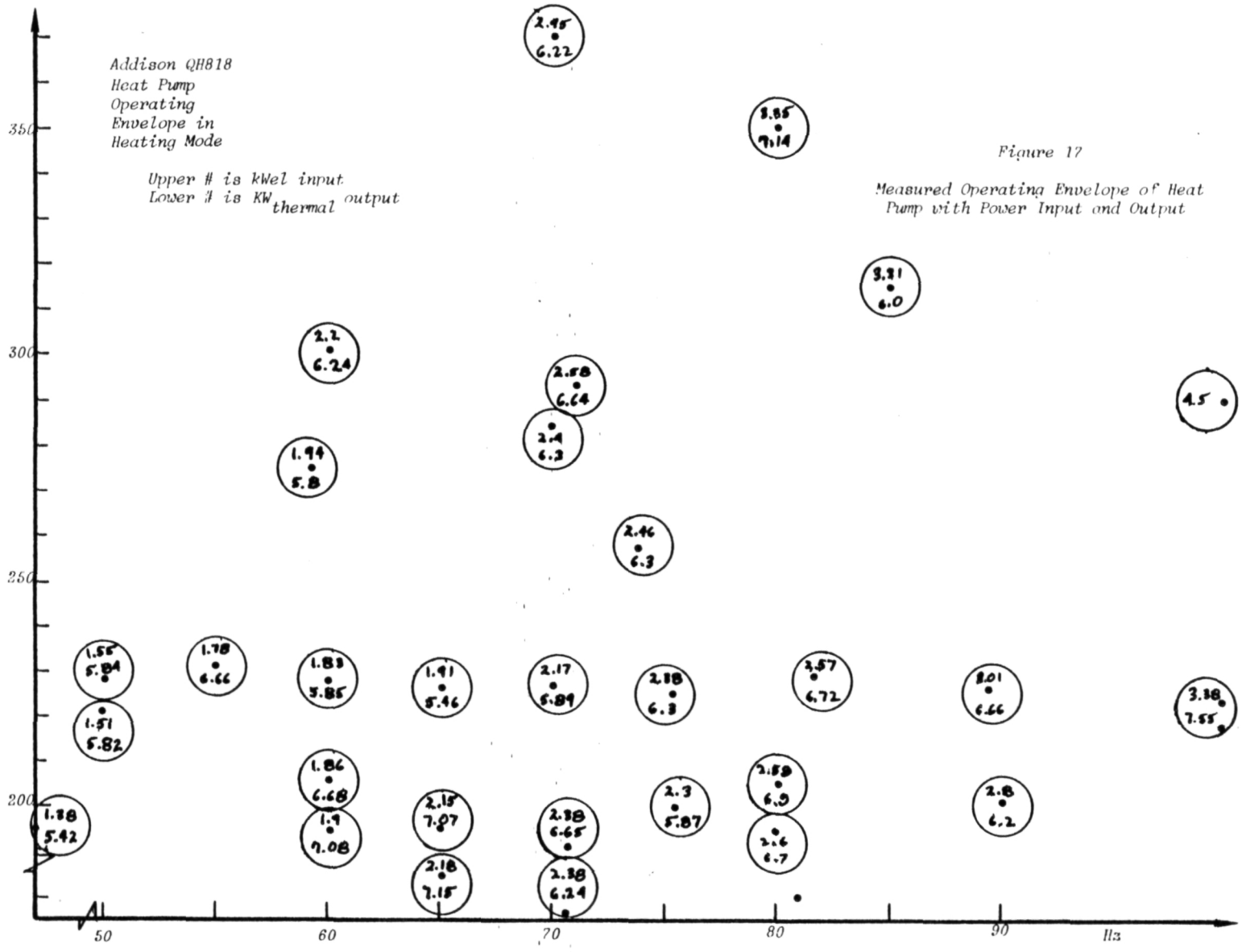

Figure 17

Measured Operating Envelope of Heat Pump with Power Input and Output

The variation in heat pump input and output power as frequency is varied is shown in Fig. 18. Note that the power output line is much flatter than the input line and the crossover is at 92% of rated frequency which support the conclusions made earlier in this section on the variation of coefficient of performance. The variation of heat pump power with voltage is shown in Fig. 19 but a reasonable linear fit of the data is unlikely. The power input data for 60 and 80 Hz have the same shape as in the 1971 tests referenced earlier. The only other test data to report is summarized in Fig. 20 where the current waveforms of the heat pump are sketched for several extreme and the nominal condition. Note the magnetic circuit saturation characteristic at high voltage and frequency and the triangular waveform due to the odd harmonics caused by excitation current at lower voltages and frequencies. These sketches were made by Dr. J. Rumbaugh, Program Manager for the DOE Wind Energy Technology Division during his site visit the last day of testing, May 21, 1985.

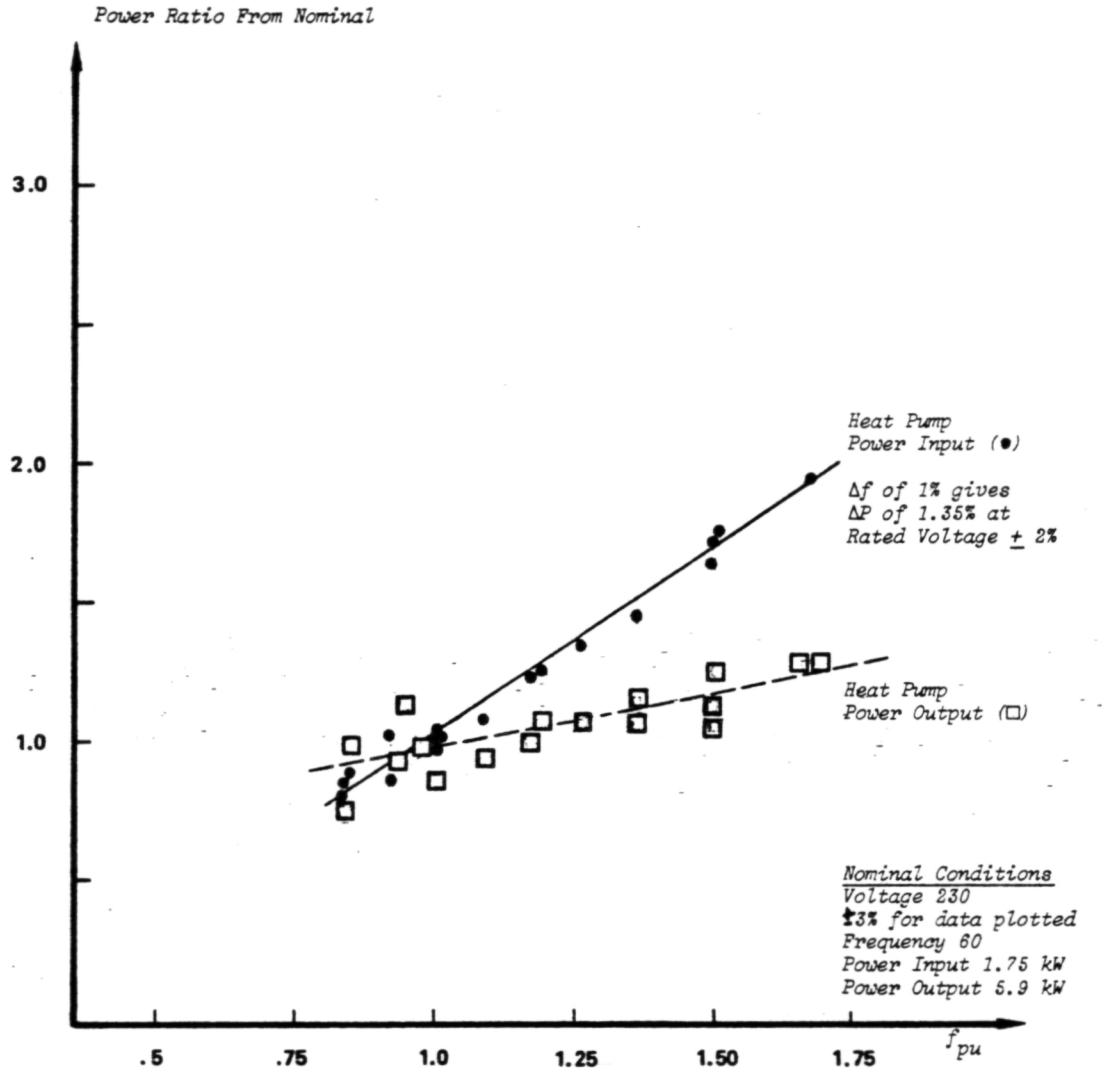

Figure 18

Variation of Heat Pump Input and Output as Frequency is Changed

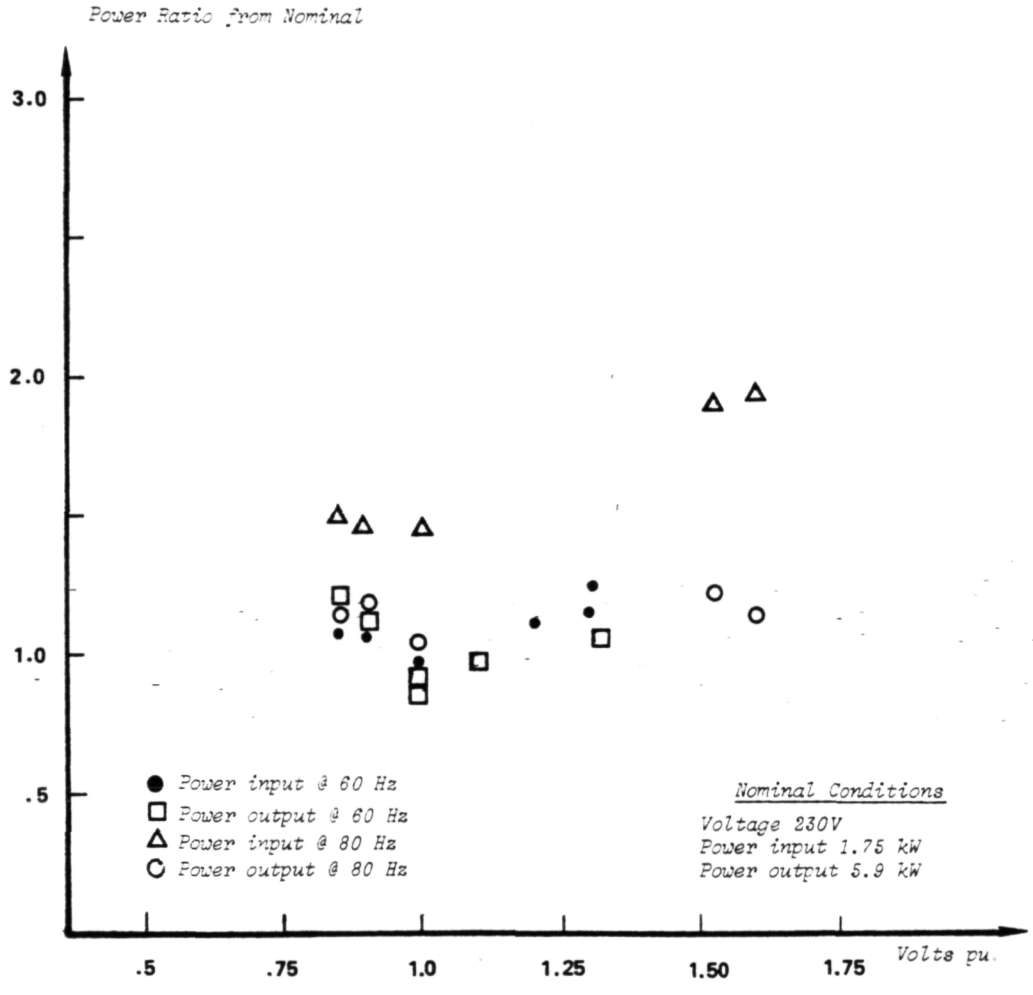

Figure 19

Variation of Heat Pump as Voltage is Changed

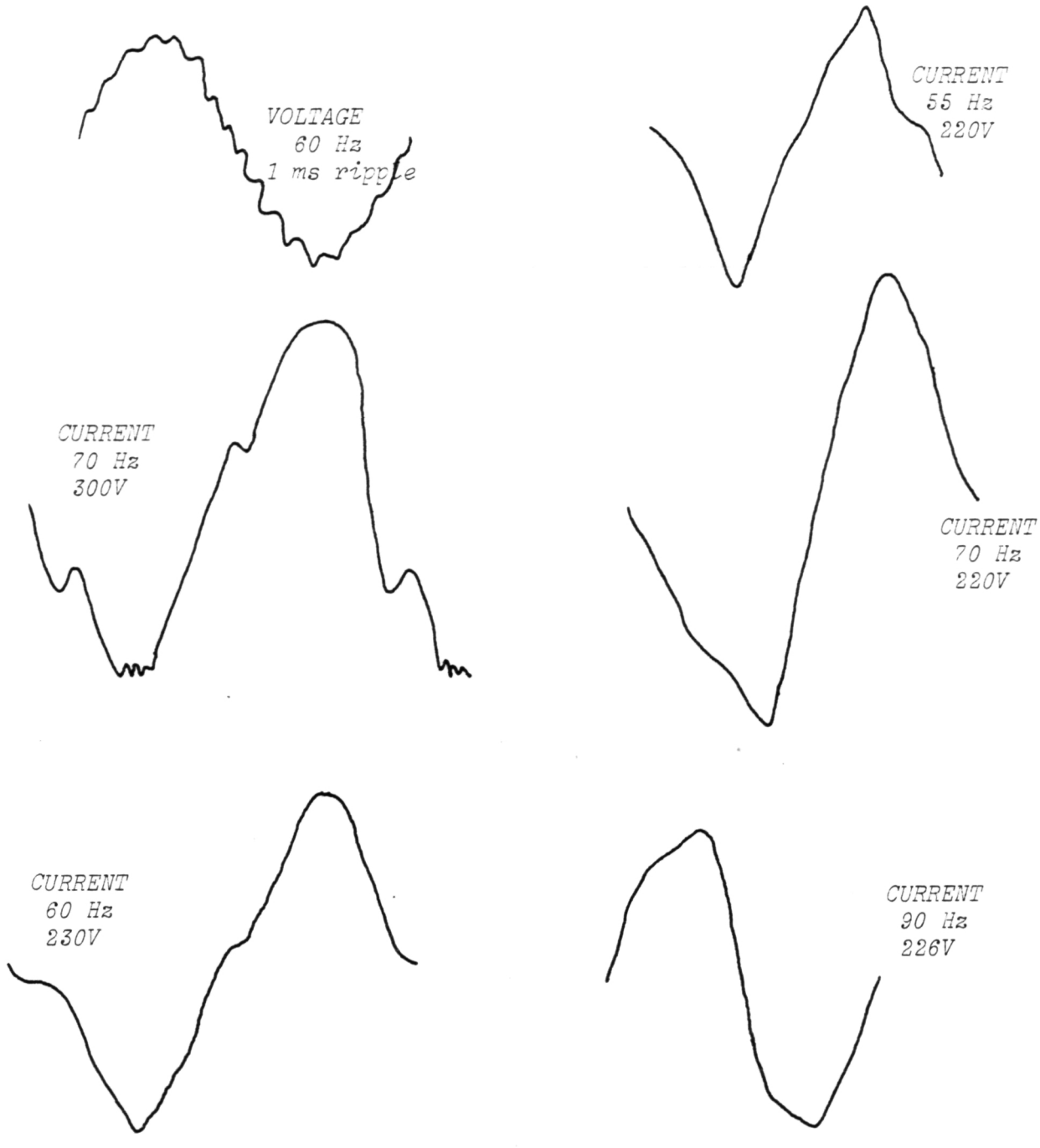

Figure 20

Current Waveforms Observed During Heat Pump Tests

VI. SIMULATION METHODOLOGY

The simulation approach chosen represents the single-phase caged motors with the classic revolving field equivalent circuit, including the start-run capacitor, as shown in Fig. 23. The pump load is modeled using the mechanical power and slip (related to motor shaft speed) variables present in the equivalent circuit. The resulting electrical and mechanical equations are then programmed on a small computer in PASCAL. The output plots from the computer runs are shown and explained in the next section.

The investigators did not have time to obtain the equivalent circuit data for the heat pump motors as well as the model of the refrigerant loop. Furthermore, not enough measurements were available to characterize that loop. Therefore, no simulation was made of the heat pump behavior. Fortunately, the input-output measurements on the heat pump were extensive so simulation was of lesser importance than with the water pumps.

1) Pump Hydraulic Loads

The experimental setups for the circulating and submersible pump tests are shown in Figures 3 and 1 respectively. Assumptions of wide open gate valves and neglect of the loss across the flow meter and the gate valve were made. The standard formulation for friction head loss in a pipe of length ℓ (ft), inner diameter D (ft) with flow Q (ft^3/sec) is

$$H_f = f \times \frac{\ell}{D} \times \frac{Q^2}{2g(D^2\pi/4)^2} \quad \text{(ft)}$$

where g is the gravitational constant and f is the Moody friction factor. The following closed form approximation [Ref. 10, p. 292] for f is

$$f = a + bR_e^{-c}$$

where

R_e = the Reynolds number = $\frac{4Q}{\pi \nu D}$

ν = the kinematic viscosity

$a = 0.094\ k^{0.225} + 0.53\ k$

$b = 88\ k^{0.44}$

$c = 1.62\ k^{0.134}$

and

k = relative surface roughness, assumed equal to 10^{-5} for plastic pipe.

The circulating pump setup has a static head of 6 feet and contains 60 ft of 1 1/4" ID plastic pipe and 345 ft. of 1" ID plastic pipe. The submersible pump setup has a static head of 28 ft. and contains 252 ft. of 1" ID plastic pipe. The sum of static and friction head theoretical loads on the two pumping setups are shown in Fig. 21.

2) Pump Models

The standard "pump curves" supplied by the manufacturer for the circulating and submersible pumps are shown in Fig. 22. In actuality, these are not truly "standard" curves as commonly used by pump manufacturers as they are not at a constant speed. Rather, they are as driven by a given induction motor which only has approximately constant speed operation. For simplicity assume that these curves are at a constant speed, the nominal operating speed at rated output of the motors, 3500 rpm for the circulating pumps and 3440 rpm for the submersible pump. These pumping curves were approximated by the closed form expression

$$H_c = 108 \left[\cos\left(\frac{\pi}{2} \frac{Q}{61}\right)\right]^{.45} \text{ ft}$$

for the circulating pump and

$$H_s = 257 \left[\cos\left(\frac{\pi}{2} \frac{Q}{26.5}\right)\right]^{.45} \text{ ft}$$

for the submersible pump. In these expressions, Q is in units of gpm. The pump efficiency curves were approximated by the closed form expression:

$$\text{eff}_c = .658 \sin\left(\frac{\pi}{2} \frac{Q}{40.5}\right)$$

for the circulating pump and

$$\text{eff}_s = .518 \sin\left(\frac{\pi}{2} \frac{Q}{16.0}\right)$$

for the submersible pump. Again Q is in gpm.

For speeds off nominal, the hydraulic affinity relationships were used to find H vs Q for points of equal efficiency to those of the equations above for H_c and H_s.

That is

$$\frac{Q}{Q_o} = \frac{f_m}{f_{mo}}$$

Figure 21

Theoretical Hydraulic Pumping Loads

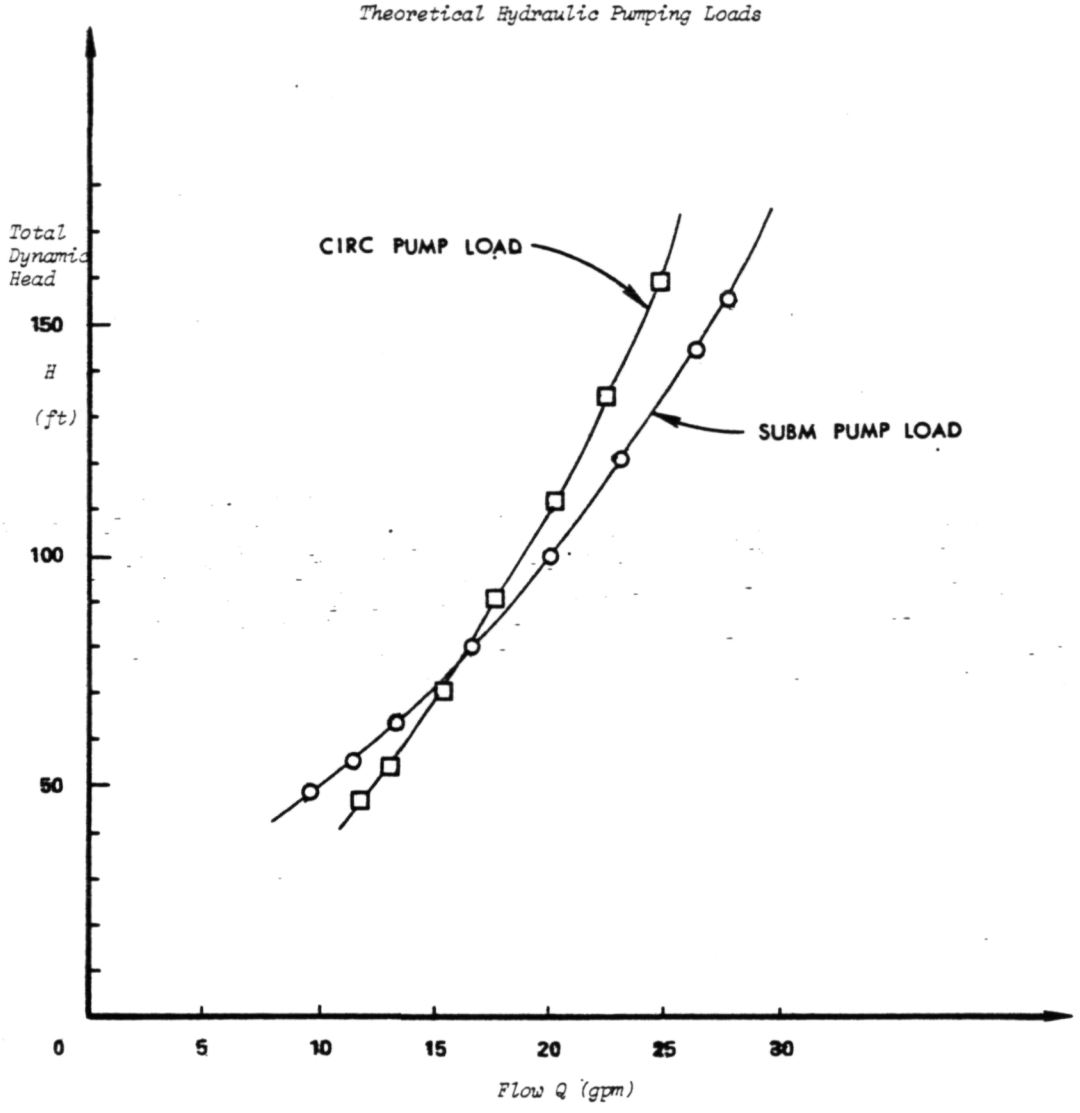

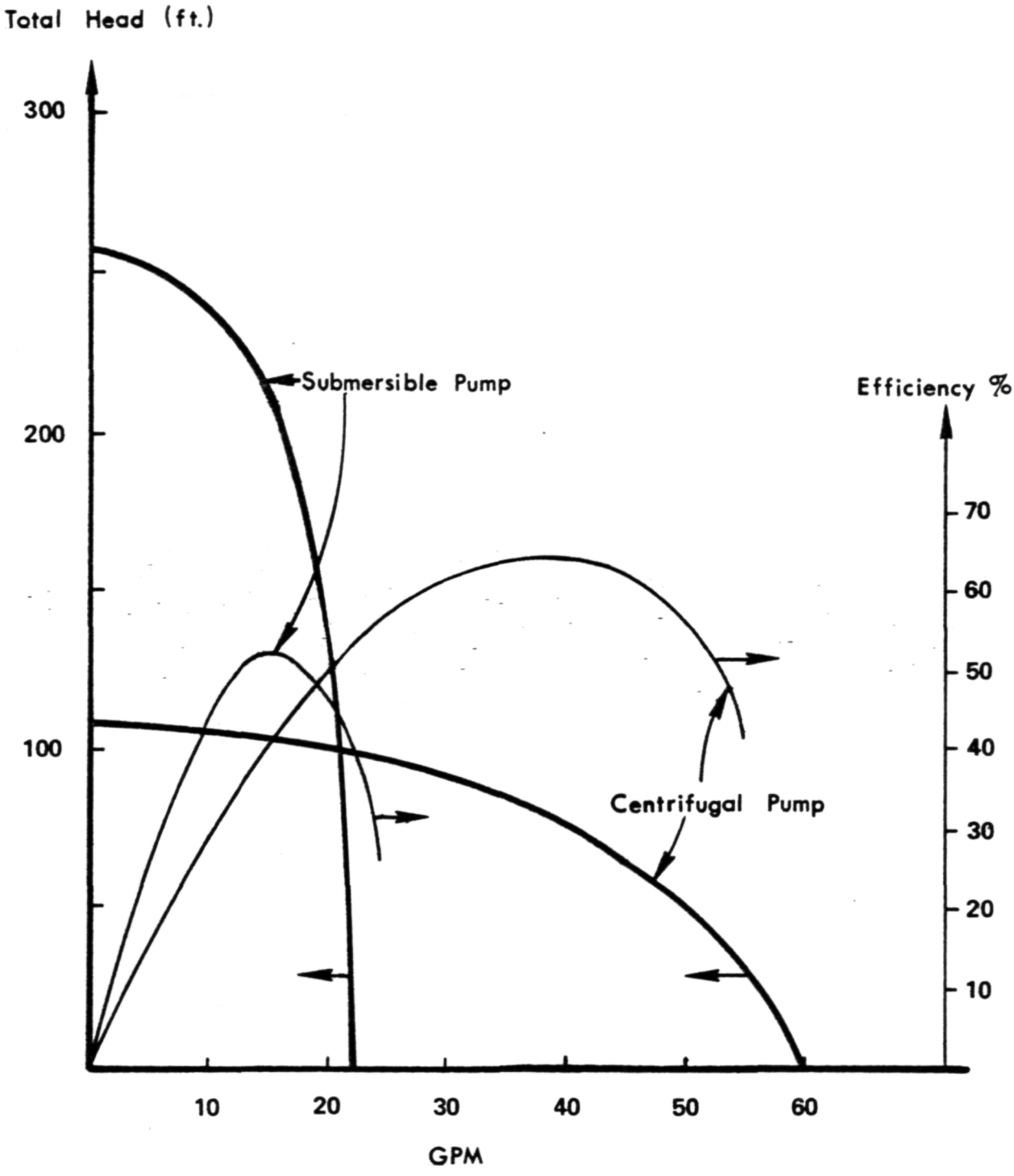

Figure 22

Pump Curves for the Water Pumps

and

$$\frac{H}{H_o} = \left(\frac{f_m}{f_{mo}}\right)^2$$

where f_m is pump speed and the subscript o refers to head and flow at the standard speed f_{mo}.

3) Pump Motor Models

Manufacturer's data for the permanent split-phase capacitor (PSC) squirrel cage induction motors supplied with the pumps used in the tests are shown in Table 2. These machines are modeled with the double revolving field theory as detailed in [Ref. 11]. The revolving field equivalent circuit derived for a PSC motor is shown in Figure 23. The input voltage sources for the forward and backward revolving fields are given by

$$V_f = V_s(1 - j/a)/2$$

and

$$V_b = V_s(1 + j/a)/2$$

where a is the effective turns ratio of the stator capacitor winding to the stator main winding and V_s is the applied RMS voltage to the electrically paralleled stator windings. The total stator input current is the phasor sum of the two stator winding forward and backward currents transformed back to their respective stationary components, and is given by

$$I_s = I_{fs}\ (1 + j/a) + I_{bs}\ (1 - j/a).$$

Thus, if V_s is the phasor reference, the input power to the motor is

$$P_{in} = V_s \times \text{Real}\ (I_s),$$

the input power factor is $PF = \dfrac{\text{Real}\ (I_s)}{|I_s|}$,

and the mechanical output power is the difference between the forward and backward powers imparted to the rotor, that is

$$P_m = 2(|I_{fr}|^2\ R_r\ \frac{1-s}{s} - |I_{br}|^2\ R_r\ \frac{1-s}{2-s})$$

where the factor of two is due to the definition of the revolving field transformation.

Table 5 is the list of equivalent circuit element values for the two water pump motors as determined by "trial and error" fitting of element

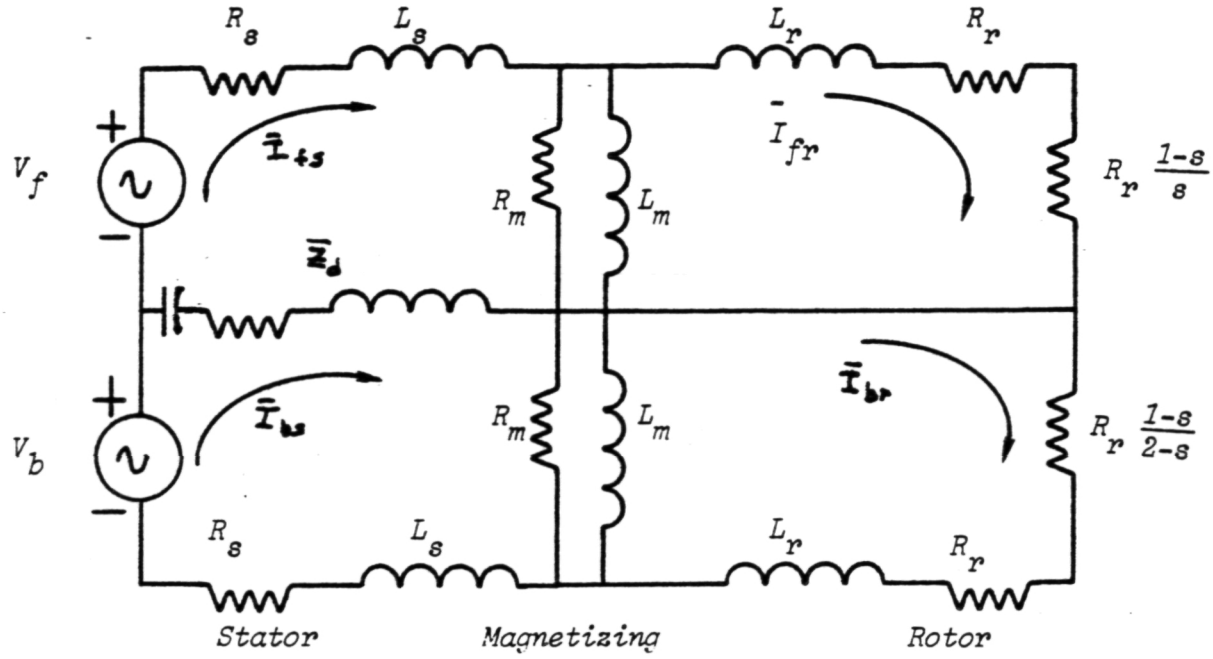

The upper loop is the forward revolving field circuit and the lower loop is the backward circuit

The parameters are:

$$Z_d = \tfrac{1}{2}(Z_{as}/a^2 - R_s - j\omega l_s) \text{ and } Z_{as} = R_{as} + j\omega L_{as} + \frac{1}{j\omega C_{as}}$$

a = *ratio of effective main stator winding turns to capacitor winding turns*

R_s = *stator main winding resistance*

R_{as} = *stator capacitor winding resistance*

L_s = *stator main winding leakage inductance*

L_{as} = *stator capacitor winding leakage inductance*

C_{as} = *start-run capacitance*

L_m = *magnetizing inductance (RTS)*

R_m = *equivalent resistance representing magnetizing losses (RTS)*

L_r = *rotor leakage inductance (RTS)*

R_r = *rotor resistance (RTS)*

s = *rotor slip* = $(f - f_m)/f$

f = *electrical supply frequency in per unit (60 Hz base)*

f_m = *mechanical speed in per unit (3600 rpm base)*

(RTS) means referred to stator

Figure 23

Equivalent Circuit for PSC Caged Motors

Element	Unit	Circulating Pump Motor	Submersible Pump Motor
a	numeric	1.25	1.25
R_s	Ω	2.43	1.814
R_{as}	Ω	4.0	3.0
$\omega_o L_s$	Ω	2.5	3.0
$\omega_o L_{as}$	Ω	3.0	3.5
$(\omega_o C_{as})^{-1}$	Ω	106	106
$\omega_o L_m$	Ω	45.0	37.0
R_m	Ω	500	225
$\omega_o L_r$	Ω	2.0	2.0
R_r	Ω	3.8	3.5
ω_o	rad/sec	377	377

Table 5

Circulating Pump Motor and Submersible Pumps
Motor Equivalent Circuit Element Values

values such that simulated performance curves matched those provided by the motor manufacturer or matched test points so provided. The equivalent circuit values in Table 5 yielded the pump motor characteristics shown in Figs. 24 and 25 where motor efficiency, speed and power factor are plotted in % against motor shaft power P_m and where motor current is in amperes.

The circuit model for motors is assumed linear so the magnetizing inductance L_m is assumed constant. As a consequence, the motor output P_m has a square-law dependence on the magnitude V_s of the stator voltage V_s given by,

$$P_m(V_s,\ f,\ f_m) = V_s^2\ P_{m1}(f,\ f_m),\ \text{where}\ P_{m1}(f,\ f_m)$$

is the mechanical output power of the motor as a function of the electrical frequency f and the shaft speed f_m, where the latter is taken at nominal input voltage of 230. V_s is in per unit (percentage of 230 volts divided by 100). For a hydraulic load of fixed configuration, the mechanical shaft speed f_m is the only independent variable in the pump and load equations. Thus it is possible to display contours of constant pump output or flow i.e.: constant pump speed due to the fixed hydraulic load configuration, on the same stator voltage-frequency plane chosen to display the operating envelope. Here specifying f_m determines pump output and pump efficiency and, indirectly, the stator voltage V_s via the equation

$$V_s = \left[\frac{\text{Pump output } (f_m)}{\text{efficiency } (f_m)\ P_{m1}\ (f,\ f_m)}\right]^{1/2} \quad \text{p.u.}$$

These contours are exhibited in the figures in the next section.

The pump output P_{pump} is only a function of the pump speed f_m but it must be determined in conjunction with the hydraulic load. Once the speed f_m has been specified, the pump head versus flow relationship is solved simultaneously with the load head versus flow relationship to find their intersection or operating point. This process for the sumbersible pump setup is shown in Fig. 26 where the intersection of the load curve with pump curve determines the total head and flow for a particular pump speed, which in this case, is the rated pump speed f_{mo}.

The sequence of calculations to generate the voltage-frequency contours indexed by flow is then as follows:

1) Specify the mechanical speed f_m.

2) Generate a new H vs Q "pump curve" for the speed f_m by use of the hydraulic affinity relationships.

3) Simultaneously solve the H vs Q "pump curve" and the H vs Q load curve for an operating point H and Q. From this point calculate the pump output power.

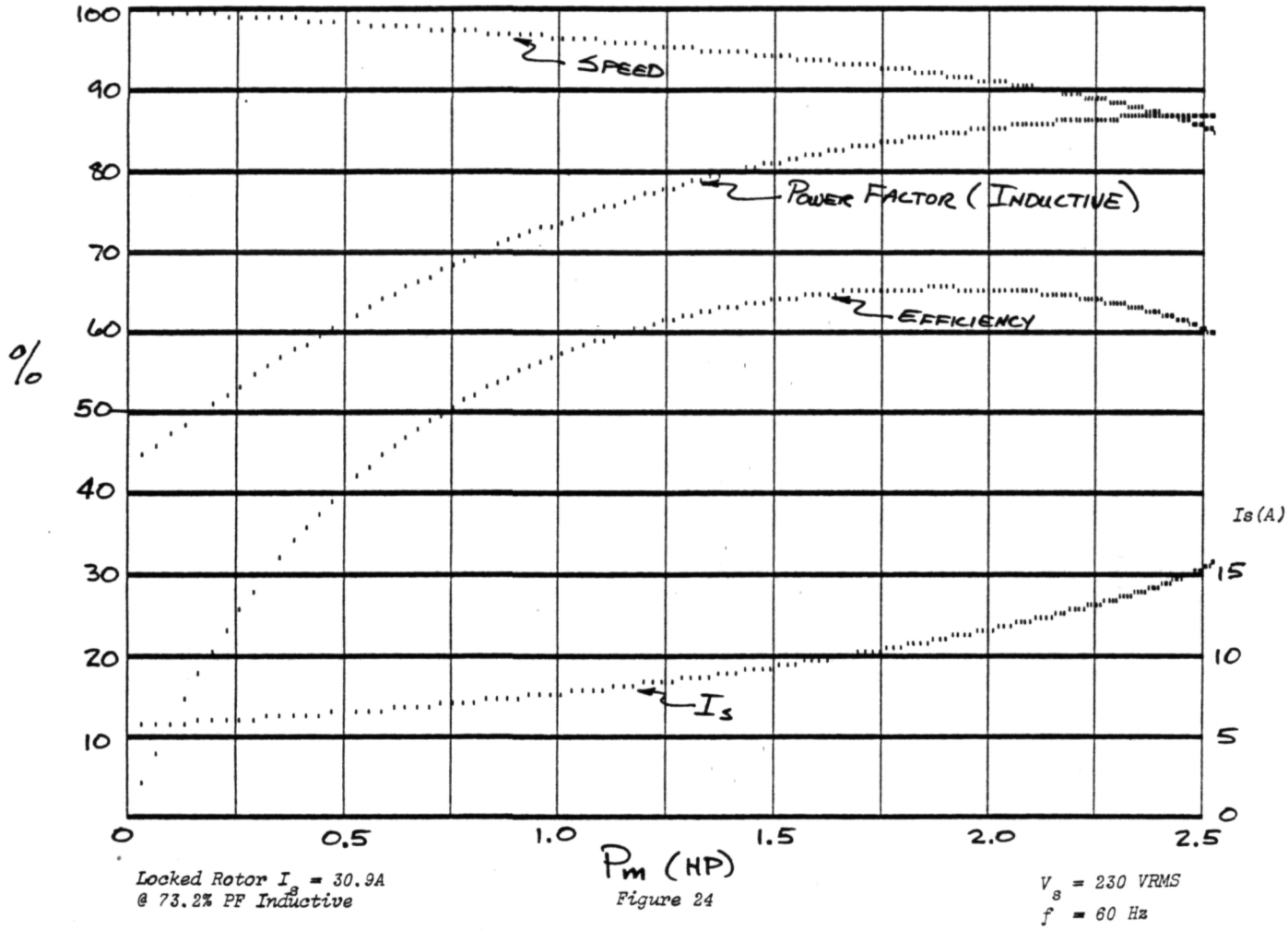

Locked Rotor I_s = 30.9A
@ 73.2% PF Inductive

Figure 24

V_s = 230 VRMS
f = 60 Hz

Submersible Pump Motor Characteristics
Generated from Equivalent Circuit

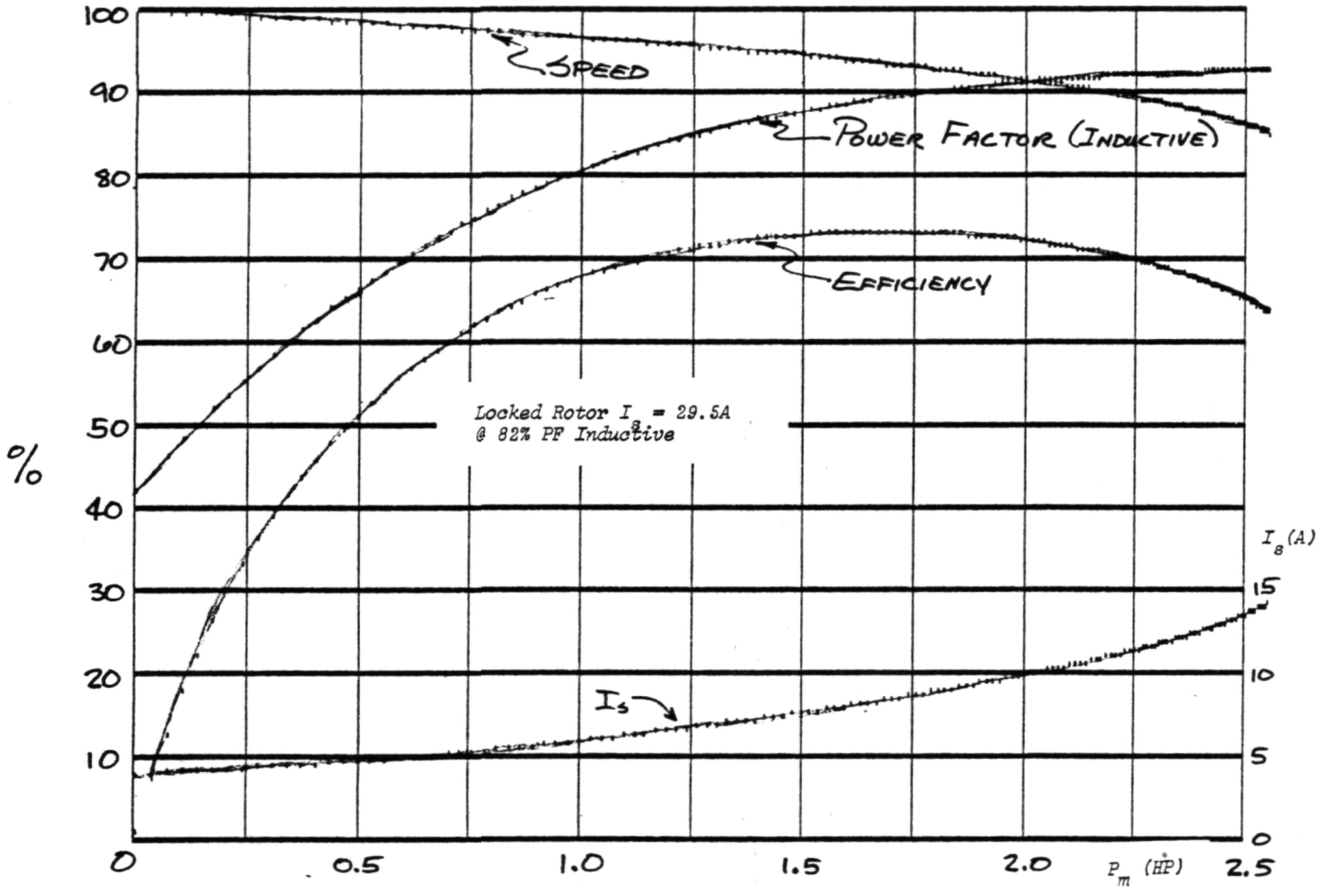

V_s = 230 VRMS
f = 60 Hz

Figure 25

Centrifugal Pump Motor Characteristics Generated from Equivalent Circuit

Figure 26

Finding Operating Point for Submersible Pump

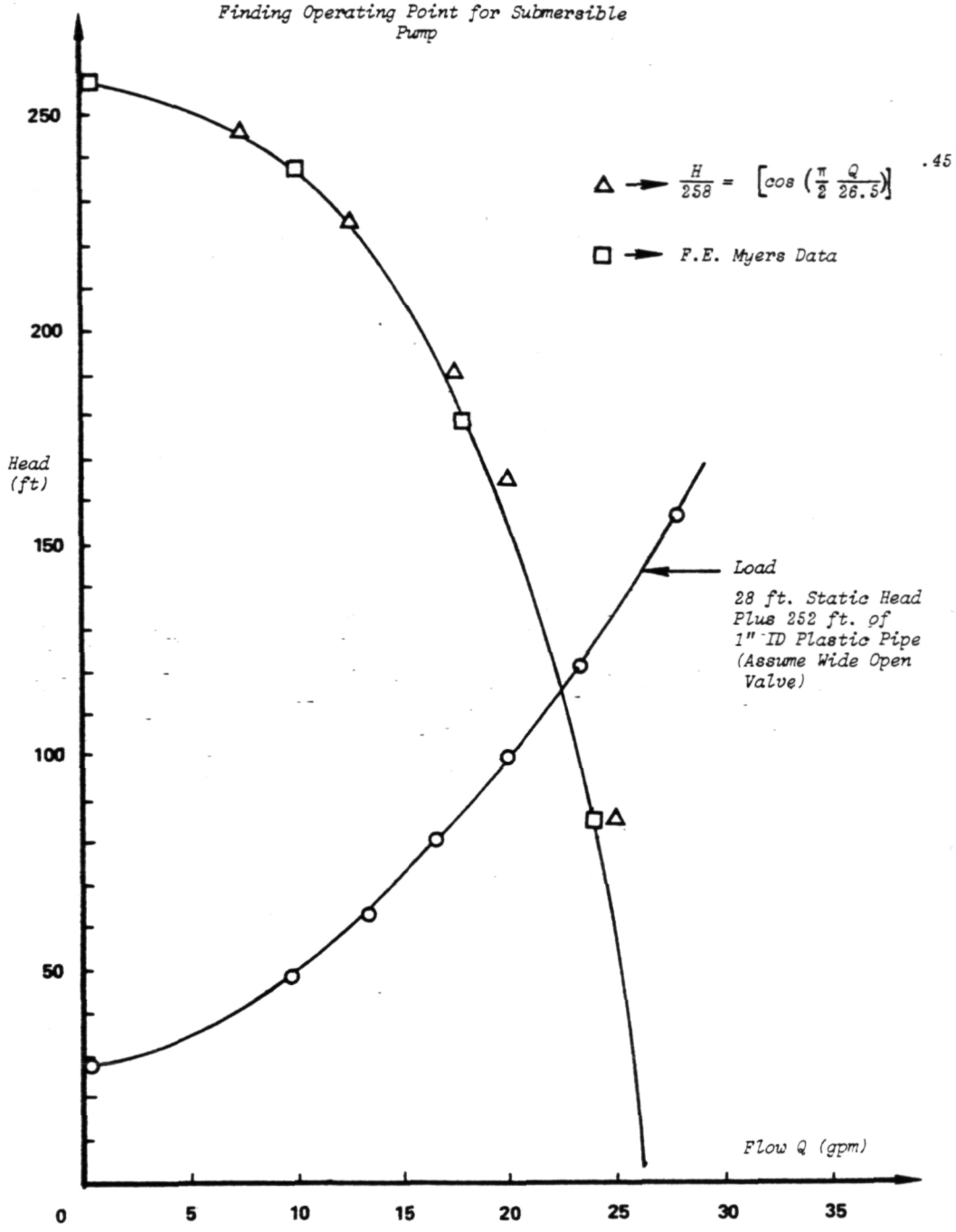

4) Determine the operating point pump efficiency from the rated speed pump efficiency curve and the hydraulic affinity relationship between flow and speed.

5) Calculate, as a function of electrical frequency f, the required motor stator voltage from the square root relationship between V_s and the pump output, pump efficiency and the motor power for rated (1 pu) stator voltage.

6) Plot the result in the V_s, f plane

VII. SIMULATION RESULTS

Calculated results for constant pump output contours in the pump voltage frequency plane are given in Figure 27. The smooth contours are labeled both in pump speed f_m and pump flow Q (gpm). As can be seen, for any speed f_m, steady-state operation is obtainable only for electrical frequencies $f > f_m$ (both f and f_m are in per unit), that is, for positive rotor slip. As f approaches f_m, the stator voltage V_s must rise as the equivalent rotor resistances also rise with decreasing slip. Conversely, as f grows above f_m the stator voltage falls, since the equivalent rotor resistances also fall with rising slip. The contours are stopped when the slip reaches 20% since for these particular motors, their torque output is maximum at that slip.

Also shown is Figure 27, are the four experimental points for which the gate valve was wide open. Correlation between theory and experiment for these four points is quite good with only the high frequency point being off by more than one gpm.

A similar set of theoretical constant pump output/speed contours for the circulating pump setup is shown in Figure 28. Here again the contours are halted at the value of electrical frequency f which gives the "pullout" slip of 20%. However, in the circulating setup there were a greater number of suitable, i.e., open gate valve, experimental points to compare to the theoretical prediction. These experimental points are also shown in Figure 28. Again, the agreement between theory and experiment is quite remarkable and again the greatest discrepancy is at the high frequency point.

Also shown in Figure 28 are two straight line contours of desired operation. One, labeled "nominal rated operation," is the desired operating locus if one had no information on the details of the operating system and the other, labeled "Max. eff. operation," is the optimum operating locus for the given fixed hydraulic load, specific pump and specific motor. This difference in operating strategies is more obvious in Figure 29 where the circulating pump motor efficiency is shown as a function of mechanical speed f_m for different electrical frequencies f. Recall that the motor model is assumed linear and as such the motor efficiency is not a function of motor terminal voltage. Operation at the maximum efficiency point for a given electrical frequency is then only a question of operating at a specific motor speed or slip. These optimum slip values are those above the maximum efficiency contour in Figure 28. This contour of optimum slips then also determines the optimum voltage divided by frequency, or V_s/f, contour for the specific pump load. If one were to operate at the nominal V_s/f ratio of unity (both V_s and f in per unit) as shown in Figure 28, the operating slip at the different values of speed can be extracted and then replotted on the efficiency curves of Figure 29. This contour clearly shows that operation at a nominal V_s/f ratio of unity is inferior, particularly so at frequencies below rated.

If one assumes an optimum wind alternator field controller, one that keeps the (V_s, f) steady-state operating contour along that shown in Figure 28, the max. eff. contour—the minimum needed pump motor input power as a function of input frequency--can be uniquely determined. This calculated input power, for

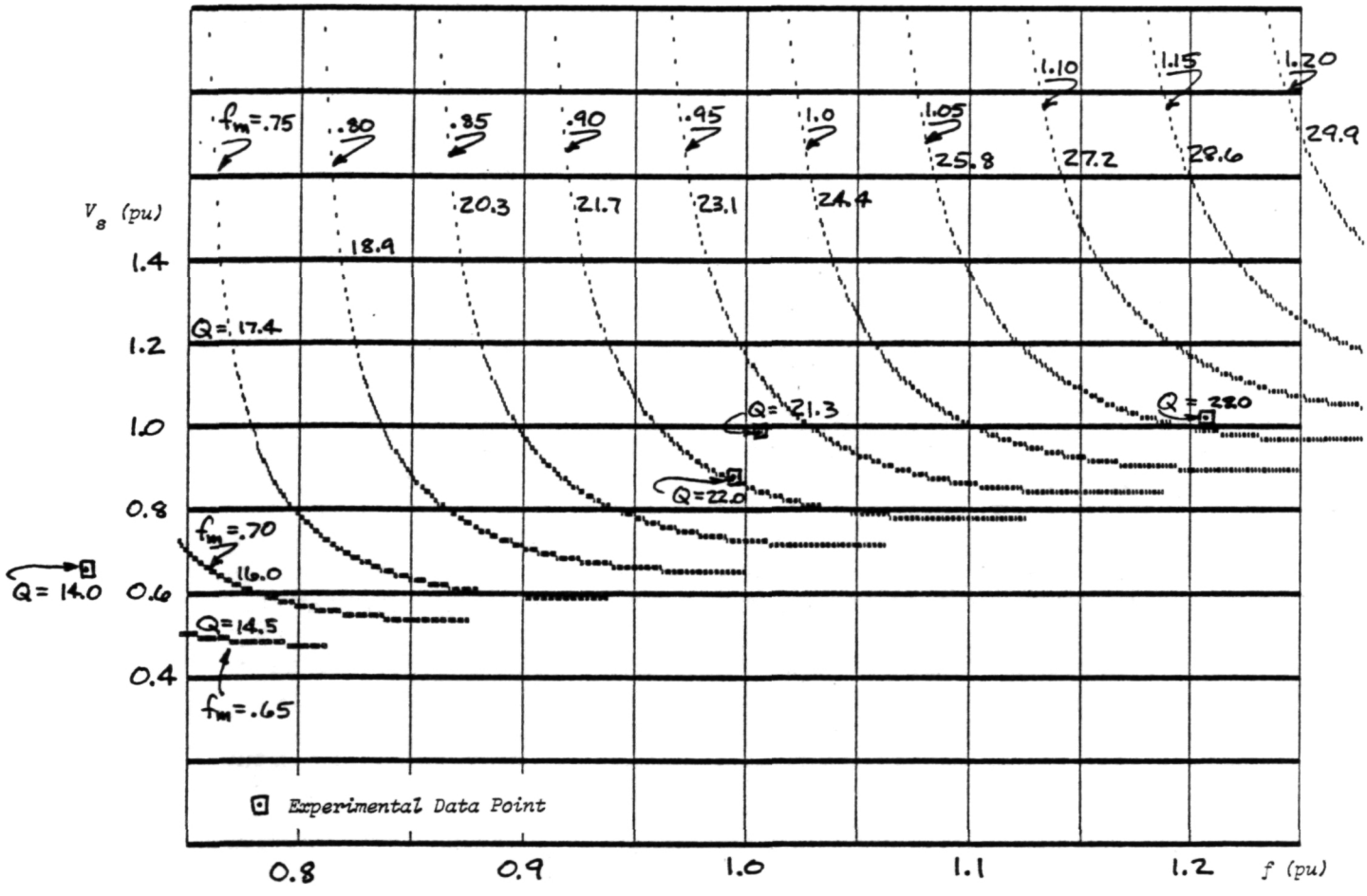

Figure 27

Simulated Voltage-Frequency Contours for Submersible Pump and Load

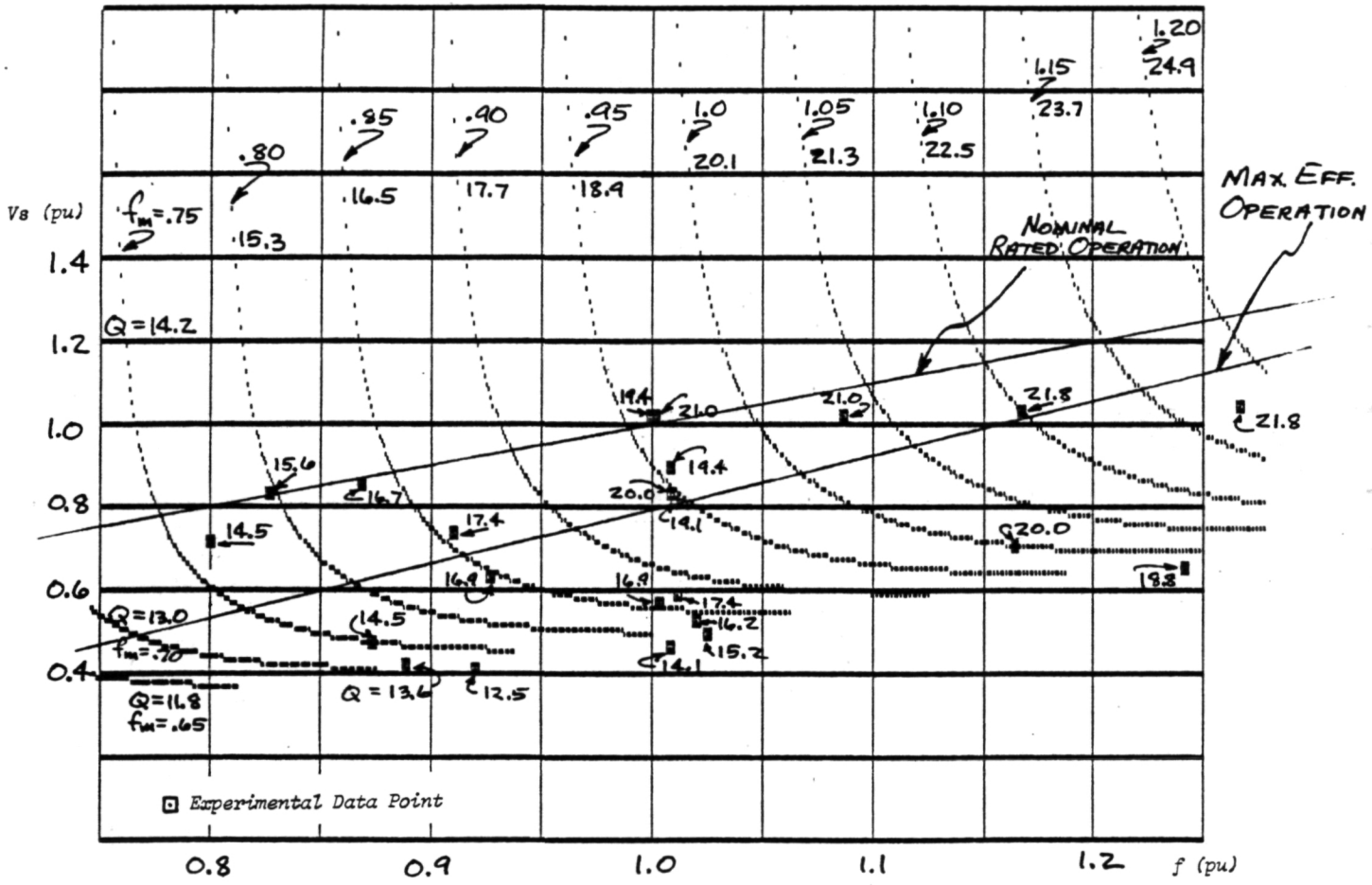

Figure 28

Simulated Voltage-Frequency Contours for Circulating Pump with Load

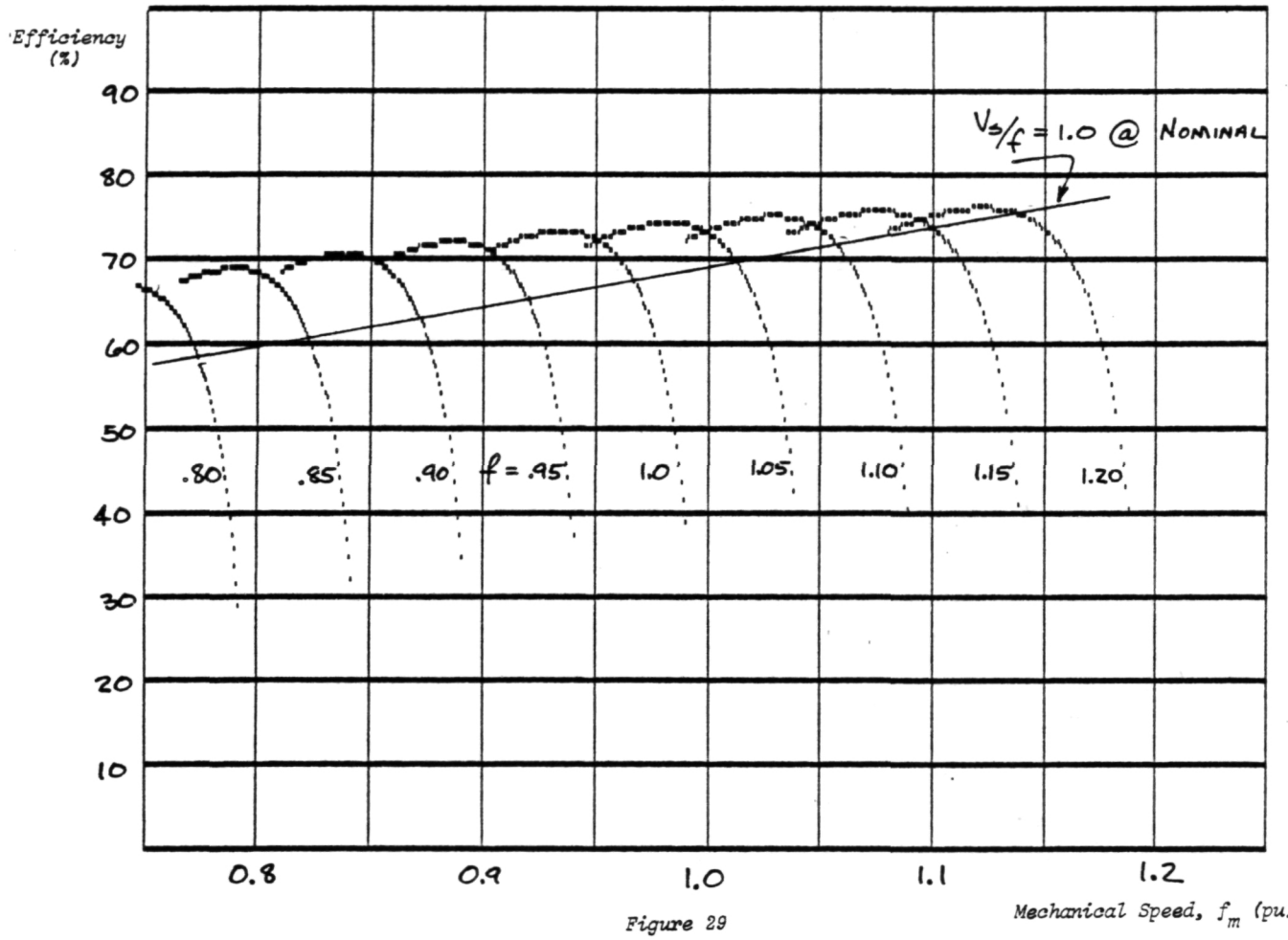

Figure 29

Simulated Efficiency vs Shaft Frequency
for the Motor in the Circulating
Pump

Figure 30

Minimum Motor Power Input vs. Supply Frequency for Circulating Pump with Long Pipe Load

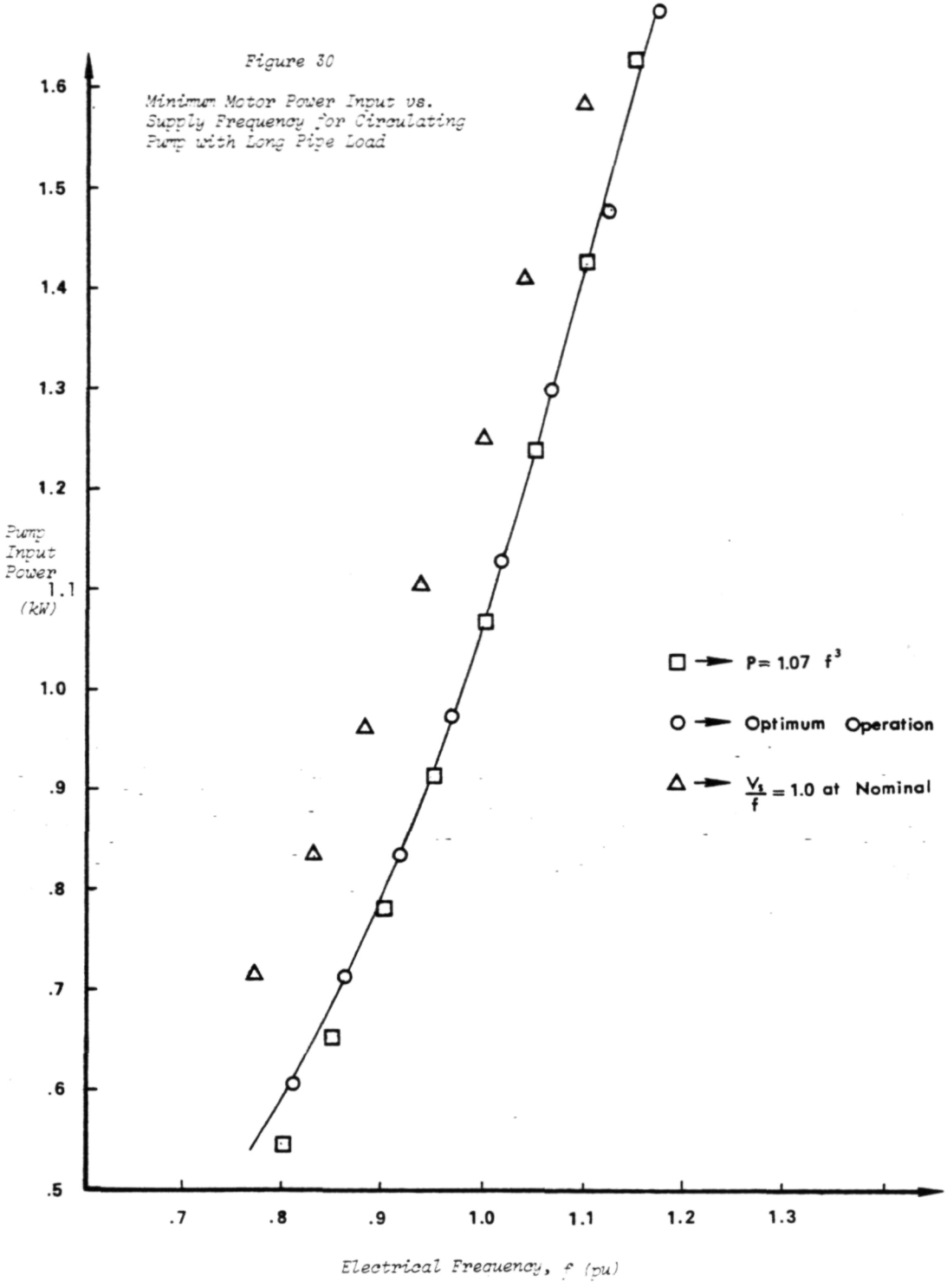

the circulating pump motor, is shown in Figure 30. Note that this minimum input power contour is a close fit to a cubic relationship in operating frequency. Since the power available from the wind is also a cubic function of the wind speed for a given swept area, this load is ideal to maintain a constant wind machine power coefficient C_p (dependent only on the ratio of wind speed to wind machine rotational speed, i.e., f for an alternator). Thus, a properly controlled alternator, induction motor, and centrifugal fluid pump working a fixed hydraulic load is an ideal wind machine load, one that enables maximum steady-state power extraction from the wind over a fixed wind speed range [Refs. 5,12].

VIII. REQUIREMENTS FOR WIND DRIVEN GENERATORS AND CONTROLLERS FOR ISOLATED OPERATION

To supply varying electrical loads with constant frequency and voltage requires generation capacity larger than the maximum load and using precise governors and a voltage control feedback system; usually including exciter feedback control, automatic tap-changing transformers and switched capacitor banks. A well-designed and operated system of several generators and many varying loads usually maintains frequency within 1% of 60 Hz and the service voltage within 5% of nominal unless there is a component failure or unless a relatively large varying load is connected. When interconnected with large utility networks, the frequency variation of a small utility as just described will significantly decrease but the voltage changes will still be approximately 5% or less. When a small controllable source, such as an isolated single generator driven by an internal-combustion engine is used, it is difficult to keep the voltage and frequency variations small unless the electrical load variables are constant. Nevertheless, a small auxilary alternator with a good governor and voltage regulator will keep voltage and frequency within the normal limits specified by most electric motor manufacturers. However, when the source of alternator power is itself highly variable, such as from a wind-electric system, then the problem of controlling frequency and voltage within tight limits becomes impossible under isolated conditions. Even when an electric windmill is interconnected to a strong utility, so that the frequency is tightly regulated, the fluctuations in wind velocity cause corresponding, but much smaller, fluctuations in local voltage while the power injected by the windmill has peak fluctuations often equal to its 15 minute average power [Ref. 9, Fig. 7]. Thus it seems reasonable to state that supplying a varying load with an isolated windmill without battery storage will result in extensive frequency and voltage variations even when sophisticated controllers and/or power conditioners are used. Since many self-excited wind-driven alternators will operate over a wind speed range of at least four to one under stand-alone or isolated conditions, it seems unlikely that shaft speed (and thus frequency) and output voltage can be held within 5% of a nominal speed without unacceptable performance compromises. This conclusion is of course the premise of this study and the reason for the tests to estimate the performance envelope of critical agricultural loads.

It is apparent from Sections V and VII that the loads considered in this study will only operate over a frequency range of approximately 50 to 90 Hz and a voltage range less than 100 to 350 volts depending upon the mechanical load characteristic. Thus, since the wind speed variations normally encountered are likely to generate voltages and frequencies that exceed the observed limits, controllers will be necessary on windmills used to feed such loads. It is important to note here that the common induction generator used in many utility-interconnected windmills requires essentially no operating controls except for a contactor. The purpose of this section is not to specify a controller for an isolated wind-driven alternator but to note some of properties of such a controller and its associated windmill suggested by the tests and analysis performed in this study.

Properties needed for voltage control:

The magnitude of the voltage across the load, which is assumed to be not far from the windmill so transmission effects can be ignored, is proportional to alternator shaft speed, magnetic flux due to field current and the turns ratio of any transformer used between alternator and load. Capacitive shunt compensation across the load can also increase voltage significantly if alternator stator inductance is large. The envelope plots in Figs. 10, 11, 13 and 14 indicate that the water pumps will operate with much less than nominal voltage at lower frequencies, although their output is higher if voltage is kept at a voltage to frequency ratio (V/f) equal to that at rated conditions (V/f = 3.8). For all devices tested above rated frequency, the control of voltage so thatV/f is held at nominal, does not increase the output significantly and leads to excessive losses and thus heating in the motor windings. This suggests a first requirement:

- The alternator field circuit (including magnetics), voltage regulator and any auto-switched transformers should be designed so the voltage is reduced as rotor speed reduces so V/f is constant below rated frequency and V is near rated above rated frequency.

Furthermore, a high and low voltage cutout function should be included if V/f control is not implemented to avoid operation at voltages below rated V/f where stalling occurs and much over rated voltage at high frequencies where motor overheating occurs. This suggests:

- Implement a high limit 20 to 30% over rated voltage and a low limit at the voltage below rated where stall due to lack of motor torque occurs.

At low frequencies, motor torque decreases due to decreased capacitor-winding current which could be compensated by increasing motor capacitance at low frequencies.

Properties needed for frequency control:

Depending upon the type of load and any capacitor switching, the load must be disconnected between 40 and 50 Hz to avoid stall and subsequent overheating. To avoid cavitation and pump overload, operation above 90 Hz is undesirable. Since normal wind speed variations at most sites will result in larger excursions in frequency, either blade pitch control or resistive loading and unloading is necessary. A resistance (heating) load could be switched in at high frequencies and switched out at low frequencies to help control the shaft speed variations.

- Implement either pitch control or controllable resistance loading to reduce the frequency range to about 50 to 90 Hz. Switch out pump loads at both high and low frequency limits and add resistive load at high frequencies to avoid rotor overspeed when the pump loads are switched out.

Fortunately, the water pump load power characteristics used increase with rotor speed in a cubic manner similar to that of rotor shaft power output so centrifugal water pump loads should not require much control within the frequency limits discussed.

Properties needed for pump starting:

Motor starting currents (locked rotor amperes) are 6 to 8 times rated currents due to motor electrical behavior and to the high inertia of the water mass or refrigerant pressure in which the pumps are immersed. There is no practical inexpensive way to unload the pumps at start without extensive modifications of the pumps as well as loss of prime and lubrication, so high starting currents must be provided by the alternator. Implementation of this function can be complex. One required electrical property of the alternator is:

- The alternator synchronous impedance (Thevenin equivalent impedance) must be low enough so the alternator short circuit current exceeds the locked rotor current of the loaded pump motor.

This requirement may prove challenging when using a large diameter many-pole alternator equal to the pump power rating which will generate 50 to 90 Hz without a speed-up gear train. Since the loads approach operating speed within a second or two, the possibility of starting with a wind gust appears attractive. This suggests a high-inertia wind rotor with a speed transducer and a control algorithm that waits until enough kinetic energy is accumulated in the rotor to start the load and still have enough speed to stay within the operating envelope of the load.

- Implement a load starting controller that monitors rotor kinetic energy until a start with subsequent operation is likely. An algorithm adapted to the local wind regime is likely needed.

Miscellaneous controller properties suggested by the tests:

- Add thermistors to motor or pump casings to disconnect loads at housing temperatures that are likely to open thermal cutouts, reduce motor life significantly, or adversely affect refrigerant-lubricant properties.

- Add an appropriate time interval to the cutout algorithm so the loads can reestablish equilibrium of the pumped fluid or gas.

Additional studies needed:

Although several pumping loads were successfully operated far outside normal voltage and frequency limits, there are several investigations necessary before the approach in this report can be recommended. They are suggested by the limitations adopted for this study:

- Transient operation with windmill source.

  The operating envelopes were determined from several-minute steady-state runs with the source at constant frequency and voltage. Using wind generation in a real wind regime will require operation of critical loads and source under transient conditions including starting and possible wind-turbine stall.

- Use of loads driven by motors with switched starting windings.

- Long-term studies estimating effects of continued large fluctuations in frequency and voltage on motor and load service life and reliability.

REFERENCES

[1] Slemon, G.R. and A. Straughen, Electric Machines, Addison-Wesley, 1980.

[2] Vosper, F.C. and R.N. Clark, "Electric Stand-Alone Water Pumping," Proceedings, Sixth Biennial Wind Energy Conference and Workshop, American Solar Energy Society, 1983, pp. 741-747.

[3] Schroeder, M.P. "Wind Systems Mechanical Heating with Pumps and Agitators," RFP-3435 [UC-60], Rocky Flats Wind Energy Research Center, Golden, CO, Aug. 1982. (available NTIS).

[4] Benaroya, A. Fundamentals and Applications of Centrifugal Pumps, Petroleum Publishing Co., Tulsa, 1978.

[5] Johnson, G.L., Wind Energy Systems, Prentice-Hall, 1985.

[6] Mullan, W., T. Gage, T. Abeles and D. Ellsworth, "Impacts of Electric Pricing Structure on Farm Load Management," NRECA Research Publication 84-A, June, 1984.

[7] Binder, R.C., Fluid Mechanics, 2nd Ed., Prentice-Hall, 1949.

[8] Park, G.L., et al, "Simulation, Estimation and Control in Power Systems," Progress Report #2, Cooperative Research Agreement between Michigan State University and Consumers Power Co., October 1, 1971.

[9] Park, G.L., O. Krauss, J. Miller, B. Weinberg, "Measuring SWECS Performance at the Owner's Site," Proceedings, Sixth Biennial Wind Energy Conference, American Solar Energy Society, Inc., June, 1983.

[10] Streeter, V.L. Fluid Mechanics, 5th ed., McGraw-Hill, 1971.

[11] Fitzgerald, A.E. and C. Kingsley, Electric Machinery, 2nd ed., McGraw-Hill, 1961.

[12] Vosper, F.C. and R.N. Clark, "Water Pumping with Autonomous Wind-Generated Electricity," paper No. 84-2602, ASAE 1984 Winter Meeting, New Orleans, Dec. 1984.

[13] Soderholm, L.H., "Optimizing Output of A Wind-Driven Alternator Using Microprocessor Control," Proceedings Windpower 1985, San Francisco, August 1985.

Appendix A

Transcription of Field Data Sheets Including Calculated Values

GPE

Data averaged over run time. * (indicates calculated quantities)

DUT	RMS Pump Voltage	Pump amps	Freq hz	Flow gpm	Pressure psi	Power in (kW)	* Apparent Power kVA	* Surface Power out (kW)	Power Factor	Gate valve	* Pump Power Out kW	Date Time	Comments
												12/3/84	
Submersible	228	9.3	60-		40	1.97	2.12	-	.93	1½ TO		1215-1222	Kohlergen
Pump	228	9.0	60-	20	40	1.88	2.05	.696	.92		.935	1232-1235	"
	228	9.25	60.4	25	40.5	1.91	2.11	.440	.905		.828	1250-1252	"
	228	9.1	60.5	21.3	18	1.9	2.075	.167	.92	Open	.429	1253-1256	"
	228	8.9	60.75	15	60	1.85	2.03	.392	.91	more closed	.526	1258:20-1259:40	"
	234	8.67	60	15.3	60.5	1.83	2.03	.403	.90	1½ TO	.542	2/21/85 1354-1409	Miller gen.
	234	9.0	60	19	40	1.87	2.11	.331	.886	1½ TO	.538	1432:10-1442:10	
	234	>12½	82			>3	>2.93					1451	
	232	10.2	65	20.3	47	2.25	2.37	.415	.95	1½ TO	.655	1458:00 - 1501:00	
	233	12.0	71	20	53	2.7	2.80	.461	.96		.699	1502:30 - 1504:30	
	233	12.0	71	22.5	53	2.7	2.80	.519	.96		.824	1505:06 - 1507:06	
	221	8.5	50.25		30	1.5	1.88		.80			1608:01 - 1610:35	
	221	19.6					4.33						locked rotor
	179	7.1	45	18.6	21	1.0	1.27	.170	.79		.370	1615	
	188	7.7	51	16	28	1.32	1.45	.195	.91		.342	1619-1620	
	170	8.1	51.5	15	27	1.27	1.38	.176	.92		.310	1620-1622	
	155				27								stall
	140				40								stall
	234	8.8	59.5	17	53.5	1.84	2.06	.396	.89		.559	1630	
	240	12.6	75	20	81	2.8	3.02	.705	.93		.941	1640	
	236	14.5	80		87	3.3	3.42		.965	60 psi @ 60 hz		2/26/85	
	231.5	9.1	60	16	60	1.85	2.11	.418	.88	set to 60 psi	.566	1226	
	194.7	7.5	48	12	36	1.1	1.46	.188	.75	from setting at above	.275		
	165		45										stall
	171	7.05	44	10.5	27	.92	1.21	.123	.76	"	.193		
	151	6.25	42	5	24	.80	.949	.052	.85	"	.079		
	150	6.4	42	6	10	.80	.960	.026	.83	opening to 10 psi	.057		
	150	6.4	42	14	8	.80	.960	.049	.83	all way open	.165		
	232	12.2	74	15	94	2.70	2.83	.613	.95	~1 TO	.747		
	233.9	12.15	73	22	60	2.70	2.84	.574	.95	more open	.855	1309	
	233.8	12.2	72.8	26	30	2.70	2.85	.339	.95	even more	.764	1311	
	233	12.0	72.3	28	21	2.65	2.80	.256	.95	all open	.756	1315	
	235.8	15.4	100	5	60		3.63	.131			.158		stall
	235.8	18.3	91.2	15-20	60	3.95	4.32	.457	.91		.637	1319	stalled @ 15-20 gpm
	236.7	16.9	85.5	23	40/60	3.7	4.00	.500±	.925		.820	1321	stall after 20 sec
	234.4	11.2	~70	22	60	2.51	2.63	.574	.95		.854		

CPE

* (indicates calculated quantities)

DUT	Pump Voltage RMS	Pump Amps RMS	Freq Hz	Flow gpm	Pressure psi	Power Input kW	* Apparent Power KVA	Surface Power out (kW)	Power Factor	Gate Valve	* Pump Power Out kW	Time EST or EDT	Comments
Submersible Pump	246	14.8	80.8	24	60.5	3.5	3.64	.632	.96		.927	2/4/85	
	204	8.8	60	13	60	1.69	1.80	.339	.94		.439	1346	
	202	8.85	60	18	40	1.69	1.79	.313	.94	open valve	.496		calibrating load
	202	8.9	59.7	21	20	1.695	1.80	.183	.94	open more	.438		
	202	8.9	59.7	22	15	1.67	1.80	.144	.93	wide open	.421		
	206	8.55	60.1	10	70	1.65	1.76	.305	.94	close valve	.371		
	208	8.15	60.1	6	80	1.60	1.70	.209	.94	close more	.240		
	232	8.62	60.0	14	60	1.75	2.00	.365	.875		.479		
	232	8.3	59.8	10	80	1.70	1.93	.348	.88	varied to get load characteristic	.414		
	232	8.72	59.9	20	40	1.80	2.02	.348	.89		.588		
	232	8.7	59.7	18	50	1.80	2.02	.392	.89		.576		
	233	8.75	59.7	22	30	1.80	2.04	.287	.88		.569		
	232	8.8	59.8	22	20	1.8	2.04	.191	.88		.469		
	235	7.0	60	35	34	1.35	1.65	.518	.82	wide open		2/26/85 1510	Stock tank load
	"			33		"						1530	2nd run
Circulating Pump	300+	10	79	64	56	2.87	>3	1.56				1550	
	271	8.75	73	47	49	2.28	2.37	1.00	.96			1620	
	257	8.45	70	41	46	2.08	2.17	.820	.96			1632	
	214	8.5	57	30	27	1.0	1.82	.352	.55			1655	
	188	6.75	46	35	23	.8	1.27	350	.63			1715	
			42										stall
	189.5	7.05	46.9	26	23	.8	1.33	.260	.60	valve open		3/27/85 1539	
	236.6	10.9	77.42	35	50		2.58	.761					New setup
	234.7	6.45	59.94	21	36	-10	1.20	1.514	.420	.79	valve open	4/30/85 1455	375' pipe load valve open
	214.4	6.15	55.28	19.35	31	-10	1.00	1.319	.345	.76		1500	
			50				pump	stalled				1506	added foot valve (2 psi)
	234	6.38	60.1	19.35	31	-10	1.20	1.493	.345	.80		1555	
	236	6.13	65.2	21.05	36	-10	1.40	1.447	.421	.97		1600	
	238	6.9	70.35	21.82	39	-10	1.59	1.642	.465	.97			
	239	7.95	76	21.82	39	-10	1.92	1.900	.465	.96		1606	125°F on motor body
	275	11.75	91.8	22.64	40	-10	3.08	3.231	.492	.95			
	206.6	5.45	60.5	19.35	31	-10	1.08	1.126	.345	.96		1623	
	192.1	5.55	60.5	20.0	31	-10	1.05	1.066	.357	.98		1624	
	186.5	5.65	60.6	19.05	30	-10	1.03	1.054	.331	.98		1626	Note ~10 psi ΔP due inlet effects
	170.4	4.85	54.6	17.39	25	-8	.80	.826	.250	.97		1635	

↑ est. for 4/9/85 runs

DUT	Pump Voltage RMS	Pump Amps RMS	Freq Hz	Flow gpm	Pressure psi	Power input kW	Apparent Power kVA	Surface Power out kW	Power factor	Gate Valve	Time	Comments
											4/30/15	
Circulating	146	5.45	55.6	16.9	25 (-8)	.80	.796	.243	1.0	open	1637	
pump	197	5.70	52.1	16.67	23 (-8)	.82	1.123	.225	.73			
	191	6.00	49.6	15.58	21 (-7)	.78	1.146	.190	.68		1654	
		stalled at 45 hz										
	164	4.55	48.0±.1	14.46	19 (-7)	.605	.746	.164	.81		1656	
	144	3.98	48.0±.2	10.81	22 (-7)	.54	.573	.130	.94	nearly closed		
	137	4.40	48				.603				1702	stalled
			100								1720	cavitated
	135	7.25	60.7±.1	17.39	27 (-9)	.98	.979	.272	1.0		1740	
	121	8.5	61.2	16.2	24 (-8)	1.00	1.029	.226	.97		1742	
	113±2	9.25±.01	61.5	15.2	21 (-7)	.95-1.05	1.045	.185	.96		1745	
	168		80.9	17.14		2.08						stalled
	151	11.6	74.5	18.75	32 (-10)	1.65	1.752	.334	.94		1750	
	162.3	9.0	69.82	20.0	35 (-11)	1.40	1.461	.400	.96		1752	
			79.8±.2			1.95						stalled windings hot
	131	7.25	60.2±.2	16.9	26 (-9)	.93	.950	.257	.98		1755	
	106	9.40	60.5	16.1	18 (-7)	.92	.996	.153	.92		1758	
	108.2	6.05	52.4±.1	14.46	19 (-7)	.64	.655	.164	.98		1802	
	96.8	7.25	53.3	13.64	17 (-6)	.66	.702	.136	.94		1804	
	93.6±1	8.5	55.2±.1	12.5	14 (-6)	.72	.796	.109	.90		1807	
	286	8.6	65.4	23.08	-15 (0)	1.50	2.460	.151	.61	open	1815	remove all
	173	4.95	55.6	21.82	-15 (0)	.72	.770	.142	.94		1817	but 30' of
	235.4	6.0	60.0±.1	23.53	-14 (0)	1.03	1.412	.143	.73		1818	1"6" ID outlet pipe acts like rotor (clogged again)

SPE

* (indicates calculated quantities)

DUT # Comments	RMS DUT Volts	RMS DUT Amps	* Apparent Power KVA	DUT Input Power KW	Freq Hz	* Power Factor	Post-fan Precoil Furnace Plenum Temp. °F	Furnace Output Temp °F	Compressor Output Temp °F	RH or Wet Bulb Temp °F or %	* Air Mass Flow lbm/min	* Furnace Output BTU/hr KW	Refrig. Temp at outside unit inlet & outlet °F	Date & Time (Setup test days clear WX)
Addison	227	7.75	1.759	1.69	60	.961	62	74	162	44	100.05	17289 5.066	150.1 65.1	5/17/85 1535 EDT
heat pump	227	7.7	1.748	1.70	59.9	.973	63	76	181		99.85	18692 5.477	162.1 66.9	1555
	227	7.7	1.748	1.7	59.7	.973	63	76	179	48	99.85	18692 5.477	161.5 66.4	1602
.30" H_2O	227	8.9	2.020	1.91	65	.946	65	78	188		99.47	18621 5.456	171.2 68.1	1604
across "A coil"	227	7.3	1.657	1.53	55.2	.923	63	76	178	50	99.85	18692 5.477	161.5 66.4	1610
fan pressure	228	7.5	1.710	1.41	50	.825	63	74	172	49	99.85	15816 4.634	155.5 65.3	1622
.62" H_2O	227	9.95	2.259	2.17	70	.961	64	78	187	49	99.66	20091 5.887	169.6 67.4	1624
in fan plenum	227	10.01	2.272	2.22	70.9±2	.977	64	79	192		99.66	21527 6.307	176.7 69.1	1629
	225	10.75	2.419	2.38	75.3	.984	64	79	193	49	99.66	21527 6.307	177.2 67.6	1631
	200	11.75	2.350	2.30	75.5	.979	66	80	203		99.29	20017 5.865	185.8 70.2	1635
	258	10.0	2.580	2.46	73.8	.954	65	80	200		99.47	21486 6.295	182.4 68.2	1637
	228	11.5	2.622	2.57	81.5	.980	65	81	205	50	99.47	22918 6.715	185.2 68.1	1642
	227	11.6	2.633	2.58	81.5	.980	66	81	203		99.29	21447 6.284	185.3 69.8	1646
stall due to lack of torque	180				81									1650
about 33 amps starting current	223	7.2	1.606	1.62	58.5	1.0(?)	64	64	99	51	startup conditions		63.5 59.1	1738
unit still in thermal	222	6.7	1.487	1.48	58.5	.995	66	75	150		99.29	12868 3.77		1743
startup transient	223	8.0	1.784	1.72	59.3	.964	67	80	163		99.10	18552 5.436	150.9 69.4	1746
	315	12.4	3.906	3.31	85	.847	69	83	183	51	98.72	19902 5.831	170.8 71.9	1751
	312	12.3	3.838	3.31	84.8	.862	68	83	195	52	98.91	21365 6.260	180.0 72.1	1753
	310	12.35	3.829	3.30	84.6	.862			201				195.3 75.6	1755
	227	12.9	2.928	2.89	89.3	.987	71	86	213	52	98.35	21244 6.224	195.3 75.6	1756
	201	14.1	2.834	2.80	90	.988	71	86	222		98.35	21244 6.224	200.9	1759
	199	13.3	2.647	2.81	89.8	1.0(?)	"	"	226		98.35	21244 6.224	204.3 75.8	1801
	276	7.92	2.186	1.94	59.2	.888	71	85	213	53	98.35	19827 5.809	193.5 74.8	1803
changed voltage & stalled due to quick voltage disconnect														
start conditions	230						61	61	61	41 (48%)	100.24		56.9 55.7	5/21/85 1134 EDT
	230	7.95	1.829	1.76	59.7	.962	63	77	168	42 (44%)	99.85	20130 5.898	150.4 66.8	1205
	284	8.9	2.528	2.4	70	.949	63	78	175		99.85	21568 6.319	162.4 67.1	1209
	284	8.8	2.499	2.4	70	.960	63	78	182	47 (43%)	99.85	21568 6.319	163.2 65.6	1214
	350	10.0	3.500	3.35	80	.957	65	82	189		99.47	24350 7.135	175.9 69.2	1217
	359	10.5	3.770	3.39	80	.899	65	81	199		99.47	22918 6.715	199.1 69.1	1220
	205	12.4	2.542	2.59	80	1.0(?)	65	81	204	49 (44%)	99.47	22918 6.715	186.8 69.5	1223
	205	12.5	2.563	2.59	80	1.0(?)	65	82	210		99.47	24350 7.135	191.0 69.9	1226
	195	13.3	2.594	2.60	80	1.0(?)	66	82	210		99.29	22876 6.703	191.0 70.5	1228
	223	15.0	3.345	3.38	996-100	1.0(?)	65	83	211		99.47	25783 7.554	188.0 69.7	1231
	218	15.6	3.401	3.41	100	1.0	65	83	230		99.47	25783 7.554	210.0 72.9	1235

compressor stall when governor jammed on attempted cool down for our lunch break!

GPE

* (indicates calculated quantities)

DUT # / Comments	RMS DUT Volts	RMS DUT Amps	* Apparent Power kVA	DUT Input power kW	Freq Hz	* Power Factor	Post fan Pre coil Furnace Plenum Temp °F	Furnace output Temp °F	Compressor output Temp °F	RH or Wet Bulb Temp °F (%)	* Air Mass Flow lbm/min	* Furnace Output BTU/Hr or kW	Refrig. Temp at Outside Unit inlet/outlet °F	Date / Time
Addison	228	8.2	1.870	1.82	60	.973	65	65	99	44 (44%)	99.47		99.0 / 74.6	5/21/95 1453 EDT
heat pump	228	8.2	1.870	1.83	60	.979	67	81	177	50 (41%)	99.10	19979 / 5.854	167.4 / 72.1	
	228	8.16	1.860	1.55	50	.833	68	82	175		98.91	19940 / 5.842	160.9 / 73.2	1514
	226	13.3	3.006	3.01	89.2	1.0	69	85	197		98.72	22745 / 6.664	185.8 / 75.6	1517
	226	13.4	3.028	2.05	90	1.0	68	86	210		98.91	25637 / 7.512	195.3 / 75.0	1523
	298	8.58	2.557	2.15	60	.841								1526
	301	8.91	2.682	2.20	60	.820	70	85	198	51 (41%)	98.54	21285 / 6.236	182.0 / 75.6	1531
	222	8.08	1.794	1.51	50	.842	70	84	188		98.54	19966 / 5.851	173.1 / 75.2	1538
close to stalling	193	7.95	1.534	1.39	47	.906	67	81	186		98.10	19979 / 5.854	171.2 / 74.0	1540
	195	8.02	1.564	1.38	47	.882	69	82	178		98.72	18489 / 5.416		1545
	stalled due to inadequate torque													
	371	9.5	3.525	2.95	90	.837	71	86	181	51 (43%)	98.35	21244 / 6.224	172.5 / 76.4	1558
	192	12.3	2.362	2.38	70.7	1.0	70	86	192		98.54	22704 / 6.652	178.4 / 76.6	1600
	294	8.92	2.622	2.58	71	.984	69	85	189		98.72	22745 / 6.664		1603
compressor motor thermal cutout opened	176	13.3	2.341	2.38	70.5	1.0	70	85	194		98.54	21285 / 6.236	185.8 / 75.1	1605
	179	13.1	2.345	3.5	readings changing	had to cool	motor	w/	sprinkling	can!				1608
	233	8.05	1.876	1.82	59.5	.970	67	67	82	52 (39%)	99.10		67.7 / 66.6	1705
	206	9.20	1.895	1.86	60	.982	68	84	157		98.91	22789 / 6.677	155.8 / 75.8	1710
motor on edge of stalling	252	7.95	1.864	1.78	55	.965	69	85	159		98.72	22745 / 6.664		1714
	244	8.06	1.967	1.76	54.8	.895	69	85	160		98.72	22745 / 6.664		1716
	195	9.9	1.931	1.90	60	.984	69	86	166		98.72	24167 / 7.081	160.7 / 77.8	1718
	195	11.0	2.145	2.15	65	1.0	70	87	171		98.54	24123 / 7.068		1720
	195	11.9	2.202	2.18	65	.99	71	88	175	51.5 (37%)	98.35	24076 / 7.054	168.5 / 79.4	1721
stopped test due to 4.5 kW into motor	205	8.5	1.743	1.69	54.1	.97	71	87	169	52 (35%)	98.35	22660 / 6.639	162.1 / 78.9	1732
	290			4.5	100									1738
Shifted to cooling (air conditioning mode) test w/ furnace plenum fan on variable freq & voltage														
			Fan power kW			A coil pressure drop								
	226	6.5	.63	1.45	60	.31" H_2O	69	56	157	53 (34%)	98.72	18480 / 5.415	66.9 / 65.7	1756
	197	7.1	.625	1.40	60	.30"	68	56	156	(35%)	98.91	17092 / 5.008	67.2 / 66.0	1758
	275	6.5	.605	1.57	60	.30"	68	56	156		98.91	17092 / 5.008	66.4 / 65.8	1800
	297	6.95	.915	2.00	70	.40"	69	57	155		115.17	19902 / 5.831		1802
2500 cfm vel	217	8.20	.900	1.78	70	.40"	69	57	162		115.17	19902 / 5.831	66.5 / 65.2	1804
.5" fan plenum near stall	238	6.30		1.34	55.5									1806
	223	6.3	.47	1.30	55	.27"	67	54	158		90.84	17006 / 4.983	65.6 / 66.7	1810
	230	6.6	.37	1.27	52	.23"	67	54			85.89	16078 / 4.711		1813
	206	6.5	.332	1.19	49	.21"	67	53	155		80.93	16316 / 4.780		1815
	stalled out @ 47 hz									(34%)				

Appendix B

PASCAL Computer Program Used for Simulation

```
{This Turbo Pascal program will perform the analysis for the centrifugal
pump psc motor, data given in Table 5, and plot on the screen the results
shown in Figure 25.  Turbo Pascal is a trademark of Borland International,Inc.}


{The following pascal functions perform network analysis.  They are roughly
based on the one-/two-port linear circuit analysis program MARTHA}

type
  vector = array[1..2000] of real; {rotating memory for complex quantities}

var
  f             :  real;
  r1,r2,r3,r4   :  integer;
  r             :  vector;
  cc1,cc2       :  integer;
  kk1,kk2       :  integer;

const
  dumi  : integer = 1;
  dumi2 : integer = 3;
  dumi3 : integer = 5;

function c1 : integer; {pointer to the real part of a complex number}
  begin
    cc1:=cc1+2; if (cc1>=199) then cc1 := 7;
    c1 := cc1;
  end;

function c2 : integer; {pointer to the real part of A of the ABCD parameters
                        of a two-port network}
  begin
    cc2:=cc2+8; if (cc2>=992) then cc2 := 201;
    c2 := cc2;
  end;

function k1 : integer;  {similar to c1 but designated keeper space}
  begin
    kk1:=kk1+2;
    if (kk1>=1199) then
      begin
        writeln('keeper counter k1 has rolled over');
        kk1:=1001;
      end;
    k1 := kk1;
  end;

function k2 : integer; {similar to c2 but designated keeper space}
  begin
    kk2:=kk2+8;
    if (kk2>=1992) then
      begin
        writeln('keeper counter k2 has rolled over');
        kk2:=1201;
      end;
    k2 := kk2;
  end;

function ca(i,j,k : integer) : integer; {complex addition}
  begin
```

```
    r[k]:=r[i]+r[j]; r[k+1]:=r[i+1]+r[j+1];
    ca := k;
  end;

function cs(i,j,k :integer) : integer;   {complex subtraction}
  begin
    r[k]:=r[i]-r[j]; r[k+1]:=r[i+1]-r[j+1];
    cs := k;
  end;

function cm(i,j,k : integer) : integer; {complex multiplication}
  begin
    r[k]:=r[i]*r[j]-r[i+1]*r[j+1];
    r[k+1]:=r[i]*r[j+1]+r[i+1]*r[j];
    cm := k;
  end;

function cd(i,j,k : integer) : integer;  {complex division}
  var dum : real;
  begin
    dum:=r[j]*r[j]+r[j+1]*r[j+1];
    r[k]:=(r[i]*r[j]+r[i+1]*r[j+1])/dum;
    r[k+1]:=(r[i+1]*r[j]-r[i]*r[j+1])/dum;
    cd := k;
  end;

function ci(i,j : integer) : integer;   {complex inverse}
  var dum : real;
  begin
    dum:=r[i]*r[i]+r[i+1]*r[i+1];
    r[j]:=r[i]/dum; r[j+1]:=-r[i+1]/dum;
    ci := j;
  end;

function cc(i,j : integer) : integer;   {complex conjugate}
  begin
    r[j]:=r[i]; r[j+1]:=-r[i+1];
    cc := j;
  end;

function cmplx(x,y : real; i : integer) : integer;  {forms a complex number}
  begin
    r[i]:=x; r[i+1]:=y;
    cmplx := i;
  end;

function zr(r : real) : integer;   {forms a resistive one-port}
  begin
    zr := cmplx(r,0.0,c1);
  end;

function zl(l : real) : integer;    {forms an inductive one-port}
  begin
    zl := cmplx(0.0,f*l,c1);
  end;

function zc(c : real) : integer;    {forms a capacitive one-port}
  begin
    zc := cmplx(0.0,-1.0/(f*c),c1);
  end;
```

```
function s(i,j : integer) : integer;  {series connection of two one-ports}
  begin
    s:=co(i,j,c1);
  end;

function p(i,j : integer) : integer;  {parallel connection of two one-ports}
  begin
    p:=cd(cm(i,j,dumi),co(i,j,dumi2),c1);
  end;

function ws(i : integer) : integer; {creates a two-port from a series
                                     connected  one-port}
  var d : integer;
  begin
    d:=c2;
    r[d]:=1.0; r[d+6]:=1.0;
    r[d+1]:=0.0; r[d+4]:=0.0; r[d+5]:=0.0; r[d+7]:=0.0;
    r[d+2]:=r[i]; r[d+3]:=r[i+1];
    ws := d;
  end;

function wp(i : integer) : integer; {creates a two-port from a shunt
                                     connected one-port}
  var d : integer;
  begin
    d:=c2;
    r[d]:=1.0; r[d+6]:=1.0;
    r[d+1]:=0.0; r[d+2]:=0.0; r[d+3]:=0.0; r[d+7]:=0.0;
    wp:=ci(i,d+4); wp := d;
  end;

function wc(i,j : integer) : integer; {cascades two two-ports}
  var d : integer;
  begin
    d:=c2;
    d:=co(cm(i,j,dumi),cm(i+2,j+4,dumi2),d);
    wc:=co(cm(i,j+2,dumi),cm(i+2,j+6,dumi2),d+2);
    wc:=co(cm(i+4,j,dumi),cm(i+6,j+4,dumi2),d+4);
    wc:=co(cm(i+4,j+2,dumi),cm(i+6,j+6,dumi2),d+6);
    wc := d;
  end;

function wts(i : integer) : integer; {terminates a two-port with a short}
  begin;
    wts := cd(i+2,i+6,c1);
  end;

function wto(i : integer) : integer; {terminates a two-port with an open}
  begin
    wto := cd(i,i+4,c1);
  end;

function wt(i,j : integer) : integer; {terminates a two-port with a one-port}
  var d,dd : integer;
  begin
    dd:=c1;
    d:=co(cm(i,j,dumi),i+2,dumi2);
    wt := cd(d,co(cm(i+4,j,dumi),i+6,dumi3),dd);
  end;
```

```
function keep1(i : integer) : integer; (puts a complex number in keeper space)
  var d : integer;
  begin
    d:=k1;
    r[d]:=r[i]; r[d+1]:=r[i+1];
    keep1 := d;
  end;

function keep2(i : integer) : integer; (puts a two-port's ABCD parameters
                                         in keeper space)
  var d,dd : integer;
  begin
    d:=k2;
    for dd:=0 to 7 do r[d+dd]:=r[i+dd];
    keep2 := d;
  end;

procedure c_initialize;  (initialize normal pointers)
  begin
    cc1:=7; cc2:=201;
  end;

procedure k_initialize;  (initialize keeper space pointers)
  begin
    kk1:=1001; kk2:=1201;
  end;


(The following are Turbo Pascal screen graphics/plotting functions
for an IBM-PC with a graphics adapter.)

var
  i,j   :integer;
  sx,sy :real;

procedure axies;
  begin
    hires;
    hirescolor(yellow);
    for i:=5 to 605 do plot(i,190,1);
    for i:=1 to 190 do plot(5,i,1);
  end;

procedure ticks1;
  begin
    for i:=1 to 10 do
    begin
      j:=5+60*i;
      plot(j,189,1); plot(j,188,1);
      j:=190-i*19;
      plot(6,j,1); plot(7,j,1);
    end;
  end;

procedure grid1;
  begin
    for i:=1 to 10 do
      begin
```

```
        for j:=1 to 600 do plot(5+j,190-19*i,1);
        for j:=1 to 190 do plot(5+i*60,j,1);
      end;
  end;


{The following is the main pascal program to analyze the psc motor.}

var
  rs,ls,ras,las,cas,lm,lr,rr,rm   : real;
  zrb,zrf,zmb,zmf,zd,zsf,zsb      : integer;
  k,m,n,x,y                       : integer;
  slip,fm,zbase,vbase,pbase,pm    : real;
  yff,yfb,ybb,ybf,vf,vb           : integer;
  a,aa,vs,pf,pb,mirf,mirb         : real;
  zm,zdf,zdb,zs,irf,irb,zo        : integer;
  isf,isb,denom,sefin,sebin       : integer;
  pein,eff,mi_line,power_factor   : real;
  im,ia,i_line                    : integer;

begin

{motor constants}
f:=1.0; rm:=500.0;
rs:=2.43; rr:=3.8;
ls:=2.5; lr:=2.0;
lm:=45.0; cas:=1.0/106.0;
ras:=4.0; las:=3.0;
a:=1.25; aa:=2.0*a*a;
vs:=230.0;

axies; grid1;
pbase:=2.5*746.0;
sx:=600; sy:=190;


for i:= 1 to 150 do
  begin
    fm:=(1000-i)/1000;
    c_initialize; k_initialize;
    slip:=(f-fm)/f;

    {setup the network shown in Figure 23.}
    zrb:=s(zl(lr),zr(rr/(2.0-slip)));
    zrf:=s(zl(lr),zr(rr/slip));
    zm:=p(zr(rm),zl(lm));
    zmb:=p(zm,zrb);
    zmf:=p(zm,zrf);
    zd:=s(s(zr(ras/aa-rs/2.0),zl(las/aa-ls/2.0)),zc(aa*cas));
    zo:=s(s(zr(ras/aa+rs/2.0),zl(las/aa+ls/2.0)),zc(aa*cas));
    zs:=s(zr(rs),zl(ls));

    {solve for the network variables}
    denom:=cs(cm(ca(zo,zmf,c1),ca(zo,zmb,c1),c1),cm(zd,zd,c1),c1);
    vf:=cmplx(vs/2.0,-vs/(2.0*a),c1);
    vb:=cmplx(vs/2.0,vs/(2.0*a),c1);
    isf:=cd(ca(cm(vf,ca(zo,zmb,c1),c1),cm(vb,zd,c1),c1),denom,c1);
    isb:=cd(ca(cm(vb,ca(zo,zmf,c1),c1),cm(vf,zd,c1),c1),denom,c1);

    im:=ca(isf,isb,c1);
```

```
      ia:=cm(cmplx(0.0,1.0/a,c1),cs(isf,isb,c1),c1);
      i_line:=ca(im,ia,c1);

      irf:=cd(cm(isf,zm,c1),ca(zm,zrf,c1),c1);
      irb:=cd(cm(isb,zm,c1),ca(zm,zrb,c1),c1);

      sefin:=cm(vf,cc(isf,1),c1);
      sebin:=cm(vb,cc(isb,1),c1);
      pein:=2.0*(r(sefin)+r(sebin));
      mi_line:=sqrt(r(i_line)*r(i_line)+r(i_line+1)*r(i_line+1));
      power_factor:=pein/(vs*mi_line);

      mirf:=sqrt(r(irf)*r(irf)+r(irf+1)*r(irf+1));
      mirb:=sqrt(r(irb)*r(irb)+r(irb+1)*r(irb+1));
      pf:=2.0*mirf*mirf*rr*(1.0-slip)/slip;
      pb:=2.0*mirb*mirb*rr*(1.0-slip)/(2.0-slip);
      pm:=(pf-pb)/pbase;

      {plot results}
      x:=5+round(pm*sx);
      y:=190-round(fm*sy); plot(x,y,1);
      y:=190-round(mi_line*sy/50.0); plot(x,y,1);
      y:=190-round(power_factor*sy);plot(x,y,1);
      y:=190-round(pm*sy*pbase/pein);plot(x,y,1);

    end;
  while not keypressed x:=1;
  end.
```